Global chromatin reorganization and regulation of genes of specific evolutionary age in differentiation and cancer

Flavien Raynal[1§], Kaustav Sengupta[2,3,4], Dariusz Plewczynski[2,3], Benoît Aliaga[1#§] and Vera Pancaldi[1,5#§]

[1]CRCT, Université de Toulouse, Inserm, CNRS, Université Toulouse III-Paul Sabatier, Centre de Recherches en Cancérologie de Toulouse, Toulouse, France.
[2]Laboratory of Functional and Structural Genomics, Center of New Technologies (CeNT), University of Warsaw, Mazowieckie, Poland
[3]Faculty of Mathematics and Information Science, Warsaw University of Technology, Warsaw, Poland
[4]Department of Molecular Genetics, Erasmus University Medical Center, Erasmus MC Cancer Institute, Rotterdam, the Netherlands
[5]Barcelona Supercomputing Center, Barcelona, Spain

[#]These two authors contributed equally to this work
[§]To whom correspondence should be addressed vera.pancaldi@inserm.fr, flavien.raynal@inserm.fr, aliaga.benoit@gmail.com

Abstract

Oncogenesis is accompanied by chromatin organization alterations and reactivation of unicellular phenotypes at the metabolic and transcriptional level. The mechanisms connecting these two observations are unexplored, despite its relevance in cancer biology.
Assigning evolutionary ages to genes in the context of 3D chromatin structure, we characterize the epigenomic landscape, expression regulation and spatial organization of genes according to their evolutionary ages. We describe topological changes across differentiation and find some of the patterns, involving Polycomb repression and RNA Pol II pausing, being reversed during oncogenesis.
Going beyond the evidence of non-random organization of genes and chromatin features in the 3D epigenome, we suggest that these patterns lead to preferential interactions of old, intermediate and young genes, mediated by respectively RNA Polymerase II, Polycomb and the lamina. Our results are in line and expand recent findings implicating loss of Polycomb repression and activation of embryonal and early evolutionary programs in cancer.

Introduction

The approximately 20,000 human coding genes emerged at different evolutionary ages and evolved together. These genes have progressively been integrated across time, adding new functions. With the genomic phylostratigraphy method, genes can be dated by looking at their homologs across species (Domazet-Lošo et al., 2007). Other methods have been proposed in the literature to estimate evolutionary gene age, such as studying duplicated genes, as demonstrated by Juan *et al*. (Juan et al., 2013). In this paper the authors highlight a correspondence between genes' ages, replication timing, breadth of expression across tissues and their propensity to accumulate copy number alterations, suggesting a scenario in which old, housekeeping genes are somehow protected from variation (both transcriptional and sequence-based) while new genes are in regions of high variability, promoting their evolvability and restricting the impacts of their evolution to specific tissues (Juan et al., 2013). The spatial organization of genes in the nucleus is also thought to play a role (Sima and Gilbert, 2014).

In 2017 Trigos *et al*. showed that the gene expression of evolutionary old genes increased in cancer, without explaining the underlying mechanism (Bussey et al., 2017; Trigos et al., 2019, 2017). Transcriptomics analyses from seven solid tumors showed that genes which originated from unicellular organisms were strongly up-regulated, and genes from metazoan origin were inactivated in cancer (Trigos et al., 2017). The increased unicellular gene expression seems to be a general phenomenon, while specific up-regulation depends on the function of the cells, suggesting that this is not a random process (Benton et al., 2021; Trigos et al., 2017). More interestingly, cancer cells show expression of genes that are specific to embryogenesis and are not expressed in healthy adult tissues (Schoenhals et al., 2009). Most cancer genes date back to the unicellular organisms and to the transition to multicellularity and complex body plans (Domazet-Lošo and Tautz, 2010; Yin et al., 2019).
These findings raised new interest in a theory that implicated the re-activation of unicellular programs in cancer, namely the atavistic theory from 1914 (Boveri, 2008), which saw the malignant tumor cell as a previously normal and "altruistic" tissue cell that changed into an "egotistical" mode with a loss of its specific functions. Evolutionary biologists hypothesize that cancer is the result of a breakdown of multicellular cooperation (Athena Aktipis et al., 2015), which is involved in the development, maintenance, and reproduction of the organism, relying mainly on epigenomic differentiation mechanisms (Henikoff, 2023). Recently, purely epigenomic mechanisms, namely the transient inactivation of Polycomb, were shown to be sufficient for the initiation of cancer in the fruit fly (Parreno et al., 2024), while embryonal programs are often implicated in dedifferentiation in cancer (Burdziak et al., 2023; Hunter et al., 2024; Patani et al., 2020) and 3D chromatin rearrangements are well

known hallmarks of cancer as they unlock phenotypic plasticity (Achinger-Kawecka and Clark, 2017; Hanahan, 2022).

Despite findings on the relationships between gene ages, expression levels and their regulation across oncogenesis, the underlying mechanisms are unclear. Both the local chromatin context and 3D organization of the genome within the nucleus have been shown to be cell type specific and to be altered during differentiation and oncogenesis, suggesting their potential role.

Recent work has shown that promoter sequence characteristics, including general GC content, TATA-box motifs and number of TF binding motifs, can be predictive of gene expression variability across tissues and individuals in multiple species (Sigalova et al., 2020), suggesting that the local chromatin environment, as well as sequence characteristics can impact expression regulation and variability.

On the other hand, the global chromatin context of genes is likely to also play a role. The 2-meter-long chain of DNA folds into 3D space and coils inside the nucleus of each cell, giving rise to several hierarchical structures, which can be different in each cell but can also globally reflect cell type and cell state (Beagan and Phillips-Cremins, 2020; Misteli, 2020). Despite consistent progress in our understanding of chromatin organization, there are still open questions about how the characteristics of the 3D epigenome can be related to cellular processes and phenotypes (Pancaldi, 2021; Papadogkonas et al., 2022; Zheng and Xie, 2019). To investigate this, a useful framework involves representing chromatin as a network in which nodes are chromatin fragments and edges are experimentally detected contacts between fragments (Pancaldi, 2023).

Here, we investigate potential local and global epigenomic mechanisms that could mediate the regulation of genes of specific evolutionary ages. We consider human embryonic stem cells, several differentiated immune cells and leukemic cells to study the gene evolutionary classes' epigenomic characteristics, their spatial patterns inside the nucleus, and their regulation across differentiation and oncogenesis. Integrating chromatin 3D structure data with epigenomic features using network approaches, we propose that different mechanisms could be responsible for the physical organization of genes of specific evolutionary ages. Specifically, ancient genes of unicellular origins and with house-keeping functions are mostly regulated and clustered by RNA polymerase 2 (PolII), intermediate metazoan genes, often involved in oncogenesis, are mostly coordinately repressed and clustered by Polycomb factors and, finally, novel mammalian specific genes, often found to be more peripheral in the nucleus, are bound and coordinately repressed by the lamina.

Results

Gene expression and expression variability are strongly associated to evolutionary ages

To explore the interplay between genes' evolutionary history, their regulation, and nuclear organization, we considered a dataset established through phylostratigraphy that assigns ages to genes based on their homologous relationships across species. The dataset comprises 19,404 genes categorized into 16 evolutionary ages, which are further grouped into three principal age classes: unicellular (UC, 7.397 genes), Early Metazoan (EM, 8.682 genes), and Mammal-specific (MM, 3.325 genes) (**Supplementary Fig. 1A**) (Trigos et al., 2017). Throughout the manuscript, we will primarily focus on the three major gene age groups for clarity and relevance in specific analyses.

We performed a functional enrichment analysis of genes within each category (**Supplementary Fig. 1B**), confirming that UC genes are enriched in fundamental cellular processes (catabolism, RNA splicing, histone modification) (Trigos et al., 2017; Yin et al., 2019). This contrasts with later phylostrata genes, which are associated with more complex cellular functions (sensory perception, keratinization). Additionally, we explored the enrichment of housekeeping genes across all age classes (**Supplementary Fig. 1C**), observing a notable proportion of UC genes classified as housekeeping compared to EM and MM genes. (18% of UC genes against 6% of EM genes and 1% of MM genes), while the EM class contains the majority of proto-oncogenes within the leukemic context (Jang et al., 2015), with some others being in the UC class. (**Supplementary Fig. 1D**).
Healthy cells display abundant variability and plasticity in their phenotype, partly based on changes in the epigenome (Ecker et al., 2018a, 2017), while expression variability can be related to cancer aggressiveness (Ecker et al., 2015). We therefore proceeded to investigate the relationship between gene age, mean expression and expression variability. Across 125 healthy individuals (Chen et al., 2016) (**Fig. 1A**, **Supplementary Fig. 1E**), our analysis revealed an inverse correlation between the 16 gene ages and average expression levels across these cell types (Spearman test, Rho = -0.95, p-value < 2.2e-16 in monocytes), indicating that older genes exhibit higher average expression levels, consistent with their involvement in fundamental cellular processes.

In the following, we define *variability* as variation of values across instances (across individuals or across single cells) and plasticity as variation in response to changes in external conditions. Briefly, Expression Variability (EV)(Alemu et al., 2014; Ecker et al., 2017) estimates the excess or reduced variability compared to what would be expected for the corresponding mean value of the feature. Since understanding expression variability is important for comprehending the underlying gene regulation mechanisms (Ecker et al., 2018b), we examined the relationship between EV and age across immune cell types. (**Fig. 1B**, **Supplementary Fig. 1F, Supplementary Fig. 1G**), observing that older genes have lower variability compared to newer genes (Spearman test, Rho = 0.77, p-value = 0.0007 in monocytes). UC genes are significantly enriched in low variability groups (groups 1 to 6) while EM genes are enriched in high variability groups (groups 8 to 10) for each of the three immune cell types considered. These results were validated when considering gene subsets with different variability but similar expression (**Supplementary Fig. 1H**).

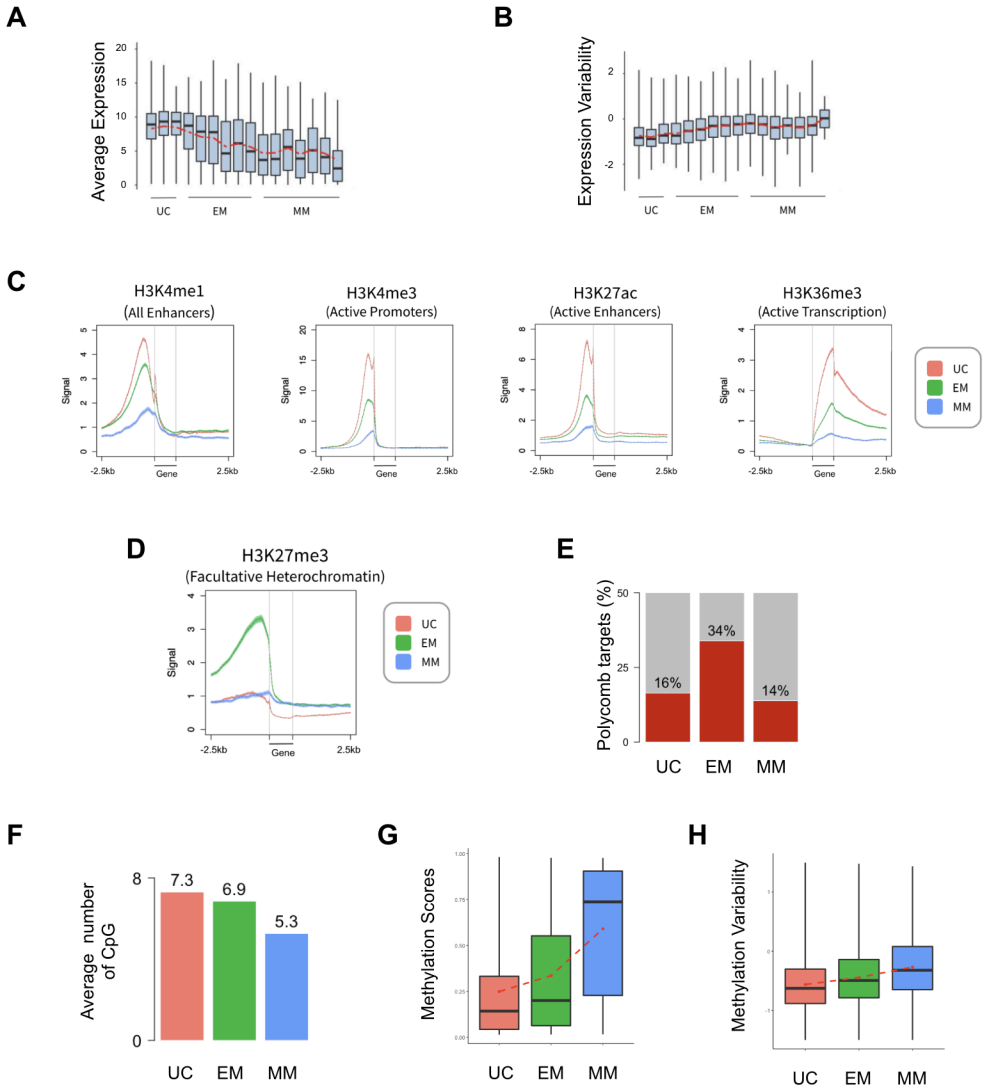

Figure 1: Genes of different evolutionary age classes display specific genomic and epigenomic features. A) Boxplot of average inter-individual gene expression levels in monocytes across 16 gene age classes (Spearman Rho = -0.95, *p*-value < 2.2e-16). **B**) Boxplot of inter-individual expression variability in monocytes across 16 gene age classes (Spearman Rho = 0.77, *p*-value = 0.00074). **C**) Average epigenetic profiles around the 3 main gene age classes (Red Unicellular genes, Green Early metazoan genes, Blue Mammal Specific genes) in monocytes. **D**) Average H3K27me3 profile around the 3 main gene age classes (Red Unicellular genes, Green Early metazoan genes, Blue Mammal Specific genes) in monocytes. **E**) Percentages of H3K27me3 repressed gene promoters in UC, EM and MM ages in monocytes. **F**) Average number of potential CpG islands by gene across the 3 main age categories in monocytes. **G**) Average Methylation scores computed by Chen *et al*. in monocytes across the 3 main age categories. Methylation scores were assigned to the 440,905 detected methylated CpG islands and calculated as the ratio between the intensity of the methylated probe and the global intensity within each individual. **H**) Average DNA methylation variability across the 3 main age categories in monocytes.

To further validate our findings, we conducted additional analyses using data from Sigalova *et al*. (Sigalova et al., 2020), which provides insights into variability across isogenic Drosophila lines and human tissues. Sigalova *et al*. identified an association between gene promoter features (sequence-based and epigenomic) in defining the level of gene expression variation. Analyzing these features related to variability in combination with the previously introduced age classes, we found correlations between gene age and active TSS (Spearman Rho = -0.37, p-value < 2.2e-16), the number of TF binding motifs in gene promoters (Spearman Rho = -0.34, p-value < 2.2e-16), the number of gene exons (Spearman Rho = -0.27, p-value < 2.2e-16), promoter size (Spearman Rho = -0.13, p-value < 2.2e-16) and GC content (Spearman Rho = -0.12, p-value < 2.2e-16) (**Supplementary Fig. 1I**).

Given the strong correlations observed among evolutionary ages, gene expression levels, and expression variability, we asked whether genes of specific age classes exhibit distinct epigenomic landscapes, which might imply different regulatory mechanisms. In monocytes, we found histone modifications associated with gene activation (H3K4me1/3, H2K27ac, H3K36me3) to be highly enriched around UC genes, intermediate intensity around EM genes and the lowest intensity in MM genes. These histone modification density levels are consistent with increasing expression levels for older genes, suggesting that the local epigenetic environment of the genes is also closely related to their evolutionary ages.

Polycomb proteins target mainly metazoan genes

We then analyzed histone modifications associated to transcriptional repression (**Fig. 1D**, **Supplementary Fig. 1J**). Interestingly, in monocytes the H3K27me3 repressive mark shows enrichment around intermediate EM genes, while both older UC and younger MM genes exhibit no enrichment, suggesting a specific regulatory role by Polycomb complexes for this gene age category. Conversely, H3K9me3 mark shows no enrichment for any gene age class.

This observation led us to focus on genes targeted by Polycomb proteins. We assessed the proportion of genes from each age class enriched with H3K27me3 peaks on the promoter in monocytes (**Fig. 1E**). Results reveal a higher proportion of EM genes (34%) targeted by Polycomb complexes whereas UC and MM genes exhibit a lower proportion of targeted genes (16% and 14%, respectively).

Taken together, these findings suggest that Polycomb protein complexes predominantly regulate genes that emerged during the metazoan period. This aligns with the role of these genes in establishing body plans and their regulated suppression in early phases of development.

CpG islands and DNA methylation variability are associated to evolutionary ages

Next, we directed our focus towards DNA methylation as a key epigenetic feature. The dataset provided by Chen *et al*. contains methylation scores for each of the 440,905 detected methylated CpG sites across the entire human genome in monocytes, gathered from 200 healthy individuals via Whole Genome Bisulfite Sequencing (Chen et al., 2016). We first investigated the genome regions associated with these methylated CpGs which showed that half of all studied CpG islands are localized around gene promoters (52.52% within 3kb of the TSS, 42% within 1kb) (**Supplementary Fig. 1K**) and explored the correlation between gene ages and DNA methylation patterns. Methylated CpG islands are thought to repress gene expression when found within promoters (Bird, 2002). Our analysis indicated a progressive decrease in the average number of CpG islands within gene promoter regions across evolutionary gene age classes (**Fig. 1F**). We then analyzed methylation scores computed by Chen *et al*. in monocyte gene promoters classified according to their respective ages. Results show a gradual increase in methylation levels for newer evolutionary ages, suggesting a preferential regulatory role of DNA methylation for MM genes (**Fig. 1G**). Interestingly, inter-individual DNA methylation variability exhibited a roughly linear increase from old to new gene age classes (**Fig. 1H**), suggesting a more stable DNA methylation profile for older genes and a more variable profile around newer genes.

Most genes deregulated through cell differentiation appeared recently in evolution

These observations led us to focus on several gene expression regulatory mechanisms that could elucidate the organization and maintenance of age-related gene expression patterns. We investigated whether these patterns remain stable across global phenotypic shifts during cell differentiation and oncogenesis.

We studied three distinct and extensively studied cell states for comparison: human embryonic stem cells (hESCs, H9), representing an undifferentiated state, differentiated cells (CD19+ primary B-cells, monocytes, neutrophils, T-cells and cardiomyocytes), and B-cells from Chronic Lymphocytic Leukemia patients (B-CLL), as a representation of a cancerous leukemic cell state (Busser et al., 2015; Ecker et al., 2017).

We first asked whether genes of specific evolutionary ages are the most regulated during cell differentiation and oncogenesis. We analyzed a gene expression dataset from hESC differentiating into cardiomyocytes (Choy et al., 2018) and computed proportions of up- and down-regulated genes within each evolutionary age class observing a predominance of up-regulated genes across cell differentiation (from 5.382 differentially expressed genes, 89% are found up-regulated), which is consistent with acquisition of a lineage specific gene expression profile (**Fig. 2A**, **Supplementary Fig. 2A, Supplementary Fig. 2B**). Interestingly, this proportion of up-regulated genes rises across evolutionary age classes (14% of UC genes, 32% of EM genes and 59% of MM genes). Conversely, a minority of genes exhibited down-regulation during cardiac differentiation, with the number of down-regulated genes being even lower for younger gene age classes (5% of UC genes, 3% of EM genes and 2% of MM genes).

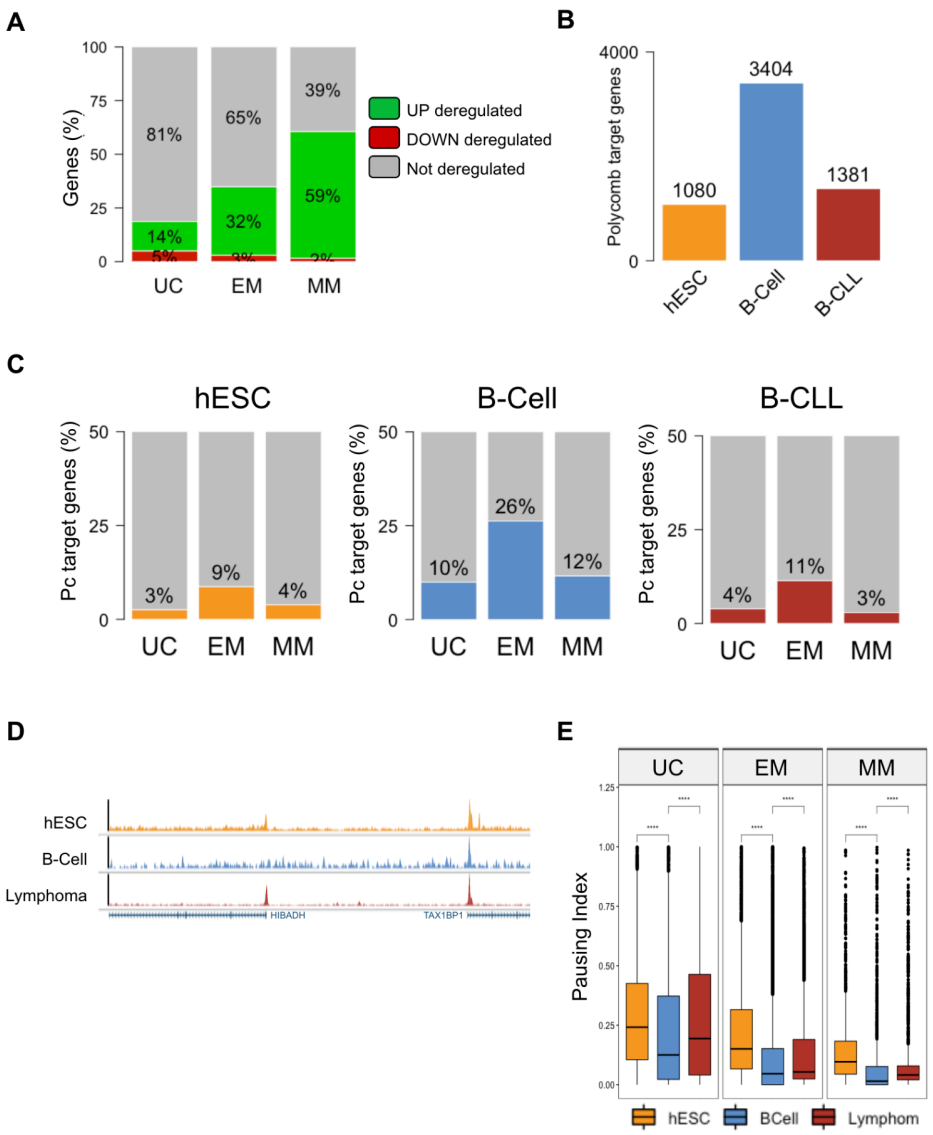

Figure 2. Gene expression regulation of different evolutionary ages is altered in differentiation and cancer.

A) Proportion of down (red), up (green) and no (grey) deregulated genes in Cardiomyocyte compared to hESC for the 3 main gene ages. **B**) Number of Polycomb target genes in hESC (yellow), B-cell (blue) and CLL (red). **C**) Percentage of Polycomb target genes for the 3 main gene age categories in hESC (left), B-cell (middle) and CLL (right) cell states. **D**) Browser snapshots of PolII tracks in hESC (yellow), B-cell (blue) and CLL (red). **E**) PolII Pausing Index distributions in hESC (yellow), B-cell (blue) and CLL (red) for each of the 3 main age groups. Statistical comparisons between groups were done by the Wilcoxon-Mann-Whitney test. n.s = not significant, **** = p<0.0001.

Gene expression regulation of genes from different evolutionary ages is altered in differentiation and cancer

In order to study how gene expression regulation is affected during cell differentiation and oncogenesis, we first focused on Polycomb protein complexes. We assessed the presence of the H3K27me3 mark in hESC, B-cell, and CLL as a proxy for Polycomb binding, which is known to repress developmentally regulated genes and influence expression noise levels (Kar et al., 2017; Kim and Kingston, 2022).
The total count of Polycomb-targeted genes across the genome was computed for each cell state, revealing an increasing number of targeted genes during cell differentiation and a sharp decline through oncogenesis (**Fig. 2B**). Building upon our earlier findings indicating that early metazoan genes (EM) were prominently regulated by Polycomb in monocyte (c.f. **Fig. 1D**, **Fig. 1E**), we observed a similar trend in stem cells, B-cells, and CLL cancer cells (**Fig. 2C**, **Supplementary Fig. 2C**), with the most notable impact of gene age class in B-cells compared to stem or cancer cells.

We then investigated gene expression regulation by RNA polymerase II (PolII) binding, another factor influencing transcription levels and variability, by analyzing Pausing RNA Polymerase II. This mechanism allows cells to modulate and synchronize transcription and can be quantified using the Pausing Index (PI) calculated as the ratio of PolII signal density around gene TSS to the PolII signal density along the gene body (Adelman and Lis, 2012).
PolII Pausing Indices were then computed for each gene in hESCs, B-cells, and B-CLL (**Fig. 2D**), and distributions were plotted for genes grouped by age class in each cell state, revealing a declining global distribution across evolutionary classes (**Fig. 2E**) and indicating that older genes are subject to tighter regulation by the PolII pausing mechanism. Interestingly, we observed significant decreases in global PolII pausing distributions during cell differentiation and significant increases during oncogenesis for every gene age class.

In summary, our findings indicate that the most recently evolved genes exhibit elevated expression levels during cell differentiation, while the oldest genes are most expressed during oncogenesis. EM genes are the primary targets of Polycomb complexes across all our cell states. Notably, the percentage of genes targeted by Polycomb seems to increase in differentiated cells and subsequently decrease in cancer. Additionally, our analysis suggests that PolII pausing is more pronounced in older genes, potentially influencing their expression regulation. With an opposite trend compared to Polycomb activity, this mechanism tends to decrease during cell differentiation and increase during carcinogenesis.

The nuclear periphery is enriched with newer genes

Gene regulation, especially through Polycomb binding, has been strongly associated with the 3D chromatin structure within the nucleus, which was shown to be deeply compromised in Polycomb units mutants (Schoenfelder et al., 2015). Chromatin organization is known to be dramatically re-organised both in cell differentiation through lineage definition (Freire-Pritchett et al., 2017), and in cancer (Deng et al., 2022; Wang et al., 2022). This prompted us to investigate whether gene evolutionary ages might also be spatially organized in the nucleus.

To explore the potential association between gene evolutionary ages and genome 3D structure, we investigated whether genes from specific age categories are more likely to be situated at the nucleus periphery. We obtained a dataset of computed Lamina Associated Domains (LADs) annotated by Kind et al. (Kind et al., 2015), across nine human cell lines, describing LADs as either facultative (cell type-specific) or constitutive (cell type-invariant).
We considered genes contained in facultative and constitutive LADs either together or separately and examined their age. Interestingly, we observed a higher proportion of younger genes associated with LAD domains (15% and 13% of MM and EM age categories, respectively) compared to older genes (7% of UC genes), (**Fig. 3A**, **Supplementary Fig. 3A**). Our findings support that genes located at the nucleus periphery are predominantly of newer origin and are consistent with the lower expression levels observed for the youngest genes (c.f. **Fig. 1A**).

Genes establish preferential contacts in the 3D chromatin network according to their age

In prior studies, we and others have demonstrated that numerous epigenomic features including many transcription factor binding peaks, gene expression, DNA methylation, histone modifications (Madrid-Mencía et al., 2020), replication timing and replication origin activation (Jodkowska et al., 2022) display strong clustering in 3D space. We used the same network framework and chromatin assortativity (ChAs) to identify which features cluster more significantly on the chromatin network than would be expected at random considering solely linear proximity of the regions along the chromosome.

We exploited promoter-centered chromatin networks derived from PCHi-C datasets, where each node represents a DNA fragment and edges signify significant physical contacts (or proximity) between DNA fragments detected by the conformation capture protocol. We started by mapping gene ages on promoter only subnetworks in monocyte, neutrophil, and T-cell (**Fig. 3B**, **Supplementary Fig. 3B**) (Javierre et al., 2016) and observed that genes from specific age classes tend to group together, forming age-specific clusters. We next confirmed this tendency using ChAs computation with the three broad gene age classes interpreted as separate binary categorical values (**Supplementary Fig. 3C**, **Supplementary Fig. 3D**) (Madrid-Mencía et al., 2020). We observed ChAs z-scores for every age category being significantly above 2 (equivalent to p-value = 0.05), indicating that contacts are more frequent than would be expected given the genomic proximity of the regions and the number of promoters in each class. Interestingly, UC genes emerge as the most assortative gene class in all three cell types, consistently followed by EM genes. Conversely, the most recent gene age category displays lower assortativity across the three immune cell types.

These findings suggest that in fully differentiated cells the oldest unicellular genes exhibit stronger connectivity among themselves, forming prominent clusters in the chromatin network, closely trailed by EM genes, which also demonstrate preferential interactions. The newest genes have less pronounced preferential interactions, with ChAs z-score values just above significance.

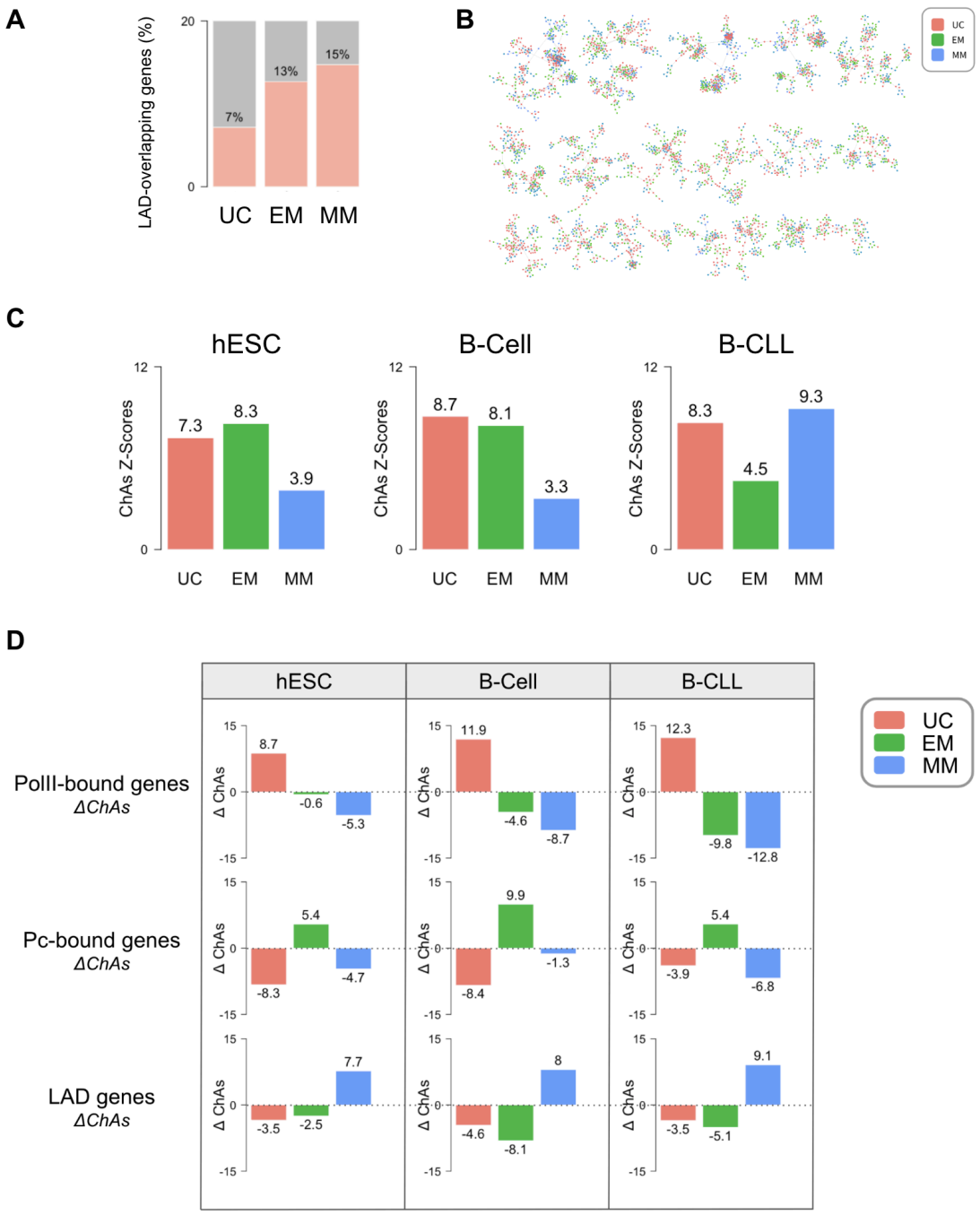

Figure 3: Spatial patterns of gene evolutionary age in 3D genome architecture. A) Overlap with Lamina Associated Domains (LADs) annotated in multiple cell lines (Kind et al., 2015) for genes belonging to the different age classes. **B**) Visualization of the 3D promoter-promoter interaction network in monocyte (Javierre *et al*. 2016) with node color representing gene age classes (red = UC, green = EM, blue = MM). **C**) Comparison of ChAs z-score of genes from different gene classes between hESCs, B-cells, and B-CLL. **D**) ΔChAs z-scores of different chromatin features: PolII (top), Polycomb (middle), and LAD (bottom) in hESC, B-Cell, and B-CLL.

Having observed specific interactions among genes of same evolutionary ages in monocyte, neutrophil, and T-cell, we next investigated the potential alteration of this age-related 3D conformational arrangement during cell differentiation and oncogenesis. We calculated ChAs z-scores on PCHi-C promoter subnetworks from hESC, normal B-cells, and cancerous B-CLL cells using the three primary age classes as binary categorical features (**Fig. 3C**). Across all cell states, we observed that each age category was significantly assortative. Notably, the oldest UC gene category consistently exhibited high assortativity values, indicating a persistent clustering tendency of these genes throughout cell differentiation and malignant transformation. Interestingly, EM genes display high ChAs values in hESC and B-Cells, and decline significantly during oncogenesis. Conversely, MM genes, which initially have the lowest values in both hESC and B-Cells, show a marked increase in clustering in CLL cancer cells. Overall, these findings indicate a substantial reorganization of interactions among both EM and MM gene groups during oncogenesis: strong clustering of EM genes is partially disrupted in cancer, while MM genes are reorganized into much stronger clusters.

So far, ChAs analysis has provided insights into chromatin features associated with 3D genome contacts, here highlighting that genes of specific ages cluster together. To further understand which specific proteins might be implicated in mediating this spatial organization, we performed a variation of ChAs analysis, denoted as deltaChAs (ΔChAs). Briefly, this method measures the difference in ChAs values obtained in subnetworks of chromatin fragments with or without a specific feature to determine whether it significantly contributes to clustering a gene group together (ΔChAs > 0) or not (ΔChAs < 0) (see Methods section for details).

We decided to test ΔChAs of several previously identified age-associated chromatin features in hESC, B-Cell, and B-CLL networks across each main age category (**Fig. 3D**). We observed positive ΔChAs for UC genes associated with PolII in all three cell types, suggesting a role of PolII in maintaining preferential contacts among UC genes in all cell states (c.f. **Fig. 3C**). The EM age class consistently exhibits positive ΔChAs z-scores for Polycomb targets compared to non-targets in all cell states, suggesting that the decrease of ChAs z-score for EM genes in B-CLL is primarily due to the disruption of preferential interactions among Polycomb-targeted EM genes which are preserved in hESC and B cells. Lastly, despite their low abundance and weaker clustering in hESC and B-cells, we observed positive ΔChAs for MM genes associated with Lamina in all three cell states. This underscores the potential importance and specificity of LAD in the clustering of genes within the MM age category across different cell states, which is especially strong in CLL cells.

Positive ΔChAs values of EM genes for Polycomb observed in all cellular states suggest that the clustering of EM genes could be mediated by Polycomb across differentiation. Other factors might be important in mediating the clustering and repression of developmental genes, specifically in stem cells. Despite the limited number of ChIP-seq datasets publicly available, we were able to calculate ΔChAs in hESC and B-cells for several TFs, showing that several of them might contribute to maintaining the clustering of UC genes and EM genes, specifically TBP, KMT2A (hESC), and STAT3 (B-Cell) for UC genes, and CTCF (hESC) for EM genes (**Supplementary Fig. 3E)**.

In the context of 3D chromatin organization, our study reveals distinctive genome spatial patterns associated with gene evolutionary ages. Further analysis identified several chromatin features responsible for the 3D clustering of each specific evolutionary age. We observed that RNA Polymerase II facilitates preferential interactions among the oldest unicellular genes, aligning with their strong and stable expression, a trend consistent across various cell states. Lamina proteins could play a role in mediating interactions of mammalian-specific genes, showing moderate clustering in hESC and B-cell, and a notable increase in CLL. Polycomb proteins modulate the assortativity of early metazoan genes, a phenomenon particularly prominent in both undifferentiated and differentiated cells compared to cancerous states. This suggests a significant reorganization of early metazoan gene interactions driven by Polycomb activity alteration during oncogenesis.

Discussion

With the purpose of investigating potential mechanisms that relate genes' evolutionary origins to their regulation and spatial organization we interrogated several datasets. Our results underscore relationships between evolutionary gene ages and several expression and epigenomic features, as well as with chromatin structure. We expand on previous observations linking gene ages to the TAD structure (Acemel and Lupiáñez, 2023; James et al., 2021; Sima and Gilbert, 2014) finding gene age to be globally assortative in chromatin networks, with particularly strong preferential clustering of genes of a particular age in specific cell states, and via regulation by potentially different mechanisms.

Given the known earlier replication timing of older housekeeping genes (Juan et al., 2013) as well as evidence of 3D organization of replication timing domains (Pope et al., 2014), of replication origin activation (Jodkowska et al., 2022) and assortativity of several chromatin states (Pancaldi et al., 2016), these findings align with existing knowledge. Indeed, polycomb

factors clearly associated with 3D structure have recently been implicated in origin activation (Prorok et al., 2023) and spatial organization of genes according to function, was suggested over a decade ago (Che et al., 2022; Cremer and Cremer, 2001; Sandhu et al., 2012; Takizawa et al., 2008) while the importance of genes' radial positioning is also well known (Bouwman et al., 2022; Misteli, 2007) and altered in cancer (Meaburn et al., 2009). We here propose hypotheses on the factors establishing this organization and how it evolves across differentiation and oncogenesis. Specifically, each gene age class exhibits distinct properties, which we will here summarize and consider in the context of relevant literature.

The oldest genes, of unicellular origin, UC, display higher expression levels, lower inter-individual expression variability, and feature active chromatin marks. Exploration of a recent characterisation of expression variability across individuals and across tissues in combination with several epigenomic features suggests that old genes would display low variability thanks to having broad promoters and multiple regulatory motifs (Sigalova et al., 2020). It is well known that the oldest genes have functions related to basic processes in the cells, (housekeeping) (Ecker et al., 2018a; Pancaldi et al., 2010; Yin et al., 2016). We find highest PolII Pausing Indexes, likely influencing their expression regulation. Interestingly, this mechanism tends to decrease during cell differentiation and increase during carcinogenesis. Previous studies demonstrated that the oldest genes, belonging to the UC age class, tend to exhibit higher gene expression levels across various solid tumor samples (Trigos et al., 2017) and were found to cluster on protein-protein interaction networks (Trigos et al., 2019). Specifically, our findings suggest that in all cell types and states the oldest unicellular genes exhibit more pronounced connectivity among themselves, forming prominent clusters in the chromatin network. Our results suggest that PolII binding is involved in clustering of UC genes while potentially maintaining coordination of their expression across differentiation and oncogenesis, in line with PolII roles in chromatin organization (Zhang et al., 2023, 2021). Despite our work focussing only on gene promoter regions, it has been recently shown that profiles of PolII intergenic binding are sufficient to cluster samples by cell line, tissue and cancer type (De Langen et al., 2023), suggesting that coordination of PolII bound genes could happen via complex networks of regulatory elements, as also suggested by analysis of PolII spatial patterns on mESC chromatin networks (Pancaldi et al., 2016). Moreover, it has been shown that establishment of replication timing in early development is impacted by PolII (Nakatani et al., 2024)

Overall our findings suggest that oncogenesis may reinstigate a balance characterized by high expression of old genes typical of undifferentiated states, which could lead to expression of ancestral and developmentally early programmes producing a shift towards unicellular phenotypes, in line with the atavistic theory (Lineweaver et al., 2021). These

would be characterized by the Warburg effect and alterations in cell-cell communication as the tissue homeostasis is disrupted.

Early Metazoan genes, EM, appeared with the evolution of multicellularity and complex body plans. They display intermediate expression and variability levels and enhanced Polycomb associated marks (H3K27me3). Polycomb protein complexes predominantly regulate genes that emerged during the metazoan period, aligning with the role of these genes in establishing body plans and their regulated suppression in early phases of development. Notably, the percentage of Polycomb targets seems to increase in differentiated cells and subsequently decrease in cancer, especially for EM genes. Those genes also demonstrate preferential interactions, but this pattern is lost in B-CLL cells, potentially in association with loss of cell identity. During development, Hox genes play a crucial role in forming the body plan (Mann and Glassford, 2024; Yamanaka et al., 2023) and rely on Polycomb group proteins for regulation (Gentile and Kmita, 2020; Kim and Kingston, 2022; Murphy and Boettiger, 2024). Moreover, numerous studies have also demonstrated that Hox genes are implicated in cancer (Brotto et al., 2020; Feng et al., 2021). Polycomb proteins could modulate the assortativity of EM genes, a phenomenon particularly prominent in both undifferentiated and differentiated cells compared to cancerous states. This suggests a significant reorganization of EM gene interactions driven by loss of Polycomb activity during oncogenesis, which was recently confirmed to produce cancers in drosophila in the absence of any genomic alteration (Parreno et al., 2024). The high value of ChAs z-score for EM genes in hESC aligns with earlier ChAs studies in mouse ESC (Pancaldi et al., 2016).

Lastly, the newest mammalian specific genes, MM, displayed higher levels of DNA methylation and methylation variability in their promoters, potentially explaining their overall lower expression level. The relationship between DNA methylation at promoters and gene expression remains poorly understood, with recent reports that sequence variants might underlie the observed negative correlation (Stefansson et al., 2024). However, the higher expression variability of new genes would be consistent with a less stable genome, accumulation of sequence variants, potentially through errors accumulated in late replication, and generally faster evolution (Juan et al., 2013). Recent peripheral enhancer regions characterized by H3K9me2 only might also play a role in regulation of MM genes (Smith et al., 2021).
Evidence from yeast also suggested a strong relation between variability of genes across single cells, across individuals, and in response to external changes (Barkai and Shilo, 2007) suggesting that genes related to immunity that have arisen more recently would display high

variability in expression and faster genomic evolution (Hagai et al., 2018; Seufert et al., 2024).

hESCs differentiation into cardiomyocytes up-regulated genes mostly in the MM class, consistent with the acquisition of a lineage specific gene expression profile.

These findings may also be attributed to the increased variability of gene expression observed across pluripotent cells; low-level expression of MM genes might be due to different cells expressing different genes in hESC. During differentiation, lineage-specific genes become upregulated in all or most cells, resulting in strong upregulation at the population level.

Interestingly, we found that genes located at the nucleus periphery enriched in the MM class. The importance of radial positioning of genes in relation to their transcriptional state has been known for close to two decades (Che et al., 2022; Takizawa et al., 2008). Given that genes interacting with nuclear lamina typically exhibit repressed expression (Reddy et al., 2008; Van Steensel and Belmont, 2017), this finding is consistent with the lower expression levels observed for the youngest genes (c.f. **Fig. 1A**). This association with the lamina might also in part explain the preferential interactions between MM genes, which is weak in stem and differentiated cells but becomes predominant in cancer, in which these genes are more strongly repressed as cell identity is lost. The effects of higher evolutionary plasticity of newer genes (Juan et al., 2013) might be controlled by their relegation to nuclear peripheral regions where they are only expressed in very specific conditions such as cancer cells. It is also possible that rewiring of chromatin in cancer alters the regulatory mode of specific gene classes, linking chromatin structure to expression noise levels via control of burst size and frequency (Seufert et al., 2024).

This work raises a series of hypotheses but we must mention several limitations of this study. First and foremost, we investigated published datasets integrating chromatin contact maps with epigenomic marks from different studies. These datasets may refer to cells in slightly different conditions and are likely influenced by biases specific to each type of experimental assay. Secondly, the chromatin assortativity measures depend, to a certain extent, on the size and characteristics of the contact networks being compared. To address this, we limited our comparisons to ChAs z-score values of gene age categories within a single chromatin network (e.g., hESC, B-cell, or B-CLL) rather than comparing across different networks. Thirdly, not all genes are present in the promoter networks, due to experimental limitations, potentially affecting our results. As a fourth point, when studying chromatin structure of cancer cells it is hard to guarantee that changes in chromatin conformation are not confounded with genome alterations. Additionally, we are here studying only the human

genome 3D structure and chromatin organization principles have changed across evolution (Hehmeyer et al., 2023; Hoencamp et al., 2021), while single-cell specific chromatin organization cannot be captured by population-aggregated data, which only informs us on global trends and might be misleading (Messina et al., 2023). Finally, another limitation is due to the lack of datasets describing promoter-centered chromatin structure in primary cancer cells, which prompted us to look at a leukemic cell instead. Differences between B-cells and B-CLL cells might be less pervasive than those between healthy cells in a tissue and their oncogenic counterparts. If solid cancer phenotypes can be related to a loss of cellular identity due to alterations of the tissue context, in leukemia the tissue context is totally absent (other than in the bone marrow and in lymph nodes). This could explain why the re-expression of UC genes is not observed in this cancer type (data not shown).

Despite these limitations, the strong relationship we observed between gene age, expression variability, regulation and 3D localisation, combined with evidence that specific genes relocate within the nucleus during oncogenesis prompts us to propose that the reshaping of chromatin during oncogenesis may modulate the variability and plasticity of phenotypes. Further work will have to be devoted to determining whether changes in the regulation of specific genes or a global rearrangement of broad gene age categories in three-dimensional space contribute to the observed alterations in variability (across cells) and plasticity (over time) during differentiation and loss of cell identity, potentially sufficient to promote oncogenesis (Frank and Yanai, 2024).

Methods

Gene Ages

We used the gene age dataset from Trigos *et al.*, which estimated gene ages through phylostratigraphy (Trigos et al., 2017). Here, 19.404 genes are classified into 16 age classes, from unicellular genes to Homo sapiens specific ones, which are grouped into three main gene age categories: Unicellular Ancestor (UC, 7.397 genes), Early Metazoan (EM, 8.682 genes), and Mammal-Specific (MM, 3.325 genes).

Expression and DNA methylation Variability

Expression and methylation variability in monocytes, neutrophils and T cells was computed from 125 healthy individuals, using a method that accounted for confounding effects due to

the correlation between mean and variability measurements (Alemu et al., 2014; Ecker et al., 2017). Fisher's exact tests were performed using the geneOverlap (v1.32.0) R package (Li Shen, 2017).

ChIP-Seq Processing

Histone modifications ChIP-Seq datasets in monocytes were downloaded from the ENCODE portal (https://www.encodeproject.org/) (Sloan et al., 2016) in BigWig format, with the ENCODE identifiers listed in Supplementary Data 1. Other ChIP-Seq datasets were downloaded in FASTQ raw format. Sequenced reads were mapped to the human reference genome (built hg19/GRCh37) using Burrows-Wheeler Aligner (bwa v0.7.17-r1188) (Li and Durbin, 2010). BAM files were obtained, sorted, and indexed by using Samtools utilities (v1.15.1) (Li et al., 2009). ChIP-Seq peak calling was performed with MACS2 (v.2.2.7.1) using the respective inputs (Zhang et al., 2008). H3K27me3 peaks were called with the --broad parameter on.

ChIP-Seq Analysis

ChIP-Seq profiles were generated using the seqplots R package (v1.23.3) (Stempor and Ahringer, 2016). Polycomb target genes were defined as genes with strict TSS localization, according to EnsDb.Hsapiens.v75 Ensembl hg19 gene annotations, that overlap with an H3K27me3 peak. CpG localizations were analyzed using the ChIPSeeker R package (v1.32.1) (Yu et al., 2015).

RNA-Seq Analysis

The raw read count matrix for hESC and hESC-derived cardiomyocytes was downloaded from GEO (accession number GSE69618) (Busser et al., 2015). Differentially expressed genes were found using the DESeq2 R package (v1.36.0), filtering for log2FC > 2 or <-2 and adjusted p-value < 0.1. Gene Ontology enrichment analysis was conducted using the limma (v3.52.1) (Ritchie et al., 2015) and clusterProfiler (v4.4.3) (Wu et al., 2021) R packages.

PolII Pausing Index

We downloaded raw RNA Polymerase II ChIP-Seq FASTQ files for hESC (H9/WA09 cell line), B-cell (GM12878 cell line), and Lymphoma B-cell (LY1 cell line) and processed them as described above. PolII BigWig density files were generated using the bamCoverage tool from deepTools suite (v3.0.2) and normalized with the --normalizeUsing RPKM flag. To compute PolII Pausing Indexes, we defined the promoter region for each gene as TSS-30bp to TSS+300bp and the gene body region as TSS+300bp to TES, based on EnsDb.Hsapiens.v75 gene annotation. PolII scores for overlapping bins within each region

were averaged separately. The Pausing Index was calculated as the ratio of PolII density in the promoter region to the density in the gene body region. Outliers in each cell's Pausing Index distribution were detected and removed using the InterQuartile Range (IQR) method. Genes with a sum of PolII Pausing Indexes across the three cell types lower than 0.2 were considered unexpressed and were excluded. Additionally, genes shorter than 1kb, according to EnsDb.Hsapiens.v75 gene annotation, were discarded. To facilitate comparison across cells, each distribution was normalized to fall between 0 and 1.

LAD-associated genes

Nuclear lamina-interacting genes were defined as genes with at least part of the gene body overlapping with LADs, according to EnsDb.Hsapiens.v75 Ensembl hg19 gene annotations and published 'constitutive' and 'facultative' LADs, either together or separately (Kind et al., 2015).

PCHi-C chromatin networks and ChAs calculations

PChi-C datasets used with GEO accession numbers are summarized in Supplementary Data 1. Considering significant interactions with CHiCAGO scores>5, we constructed networks by considering DNA restriction fragments as nodes and interaction between fragments as edges. These networks were processed using the igraph R package (v1.3.2) (Csárdi et al., 2023). Chromatin Assortativity was calculated using the ChAseR R package (v0.0.0.9) (https://bitbucket.org/eraineri/ChAseR/) (Madrid-Mencía et al., 2020). Gene age ChAs was computed using age classes in the categorical ChAs mode. For z-score calculations, we performed 100 randomizations preserving genomic distances (dist.match = TRUE). Chromatin networks were visualized using Cytoscape (v3.8.0) and Gephi (v0.10.1).

ΔChAs calculation

We developed the ΔChAs method to identify chromatin features associated with the 3D clustering of specific gene groups (e.g., age categories) by determining whether these features significantly contribute to clustering a gene group together (ΔChAs > 0) or not (ΔChAs < 0). Within each category, two gene subgroups are created based on the presence or absence of a chromatin feature. ChAs z-scores for both subgroups are then calculated. Finally, ΔChAs is determined as the difference between the ChAs z-score of genes associated with the specific feature and the ChAs z-score of other genes.

Data availability

No new data was produced for this study. The full list of previously published datasets used in this study is provided in **Supplementary Data 1**.

Code availability

The code used for analysis and to generate main figures is accessible at https://github.com/VeraPancaldiLab/Gene-Ages-Paper/. Processed datasets required to run the R script properly can be found at https://github.com/VeraPancaldiLab/Gene-Ages-Paper/tree/main/Datasets.

Acknowledgments

The authors thank Michael N. Kammer, Daniel Rico, and David Juan for the critical reading of the manuscript.

Author Contribution

F.R, B.A. and V.P. designed the study. B.A. provided knowledge and background of the study. F.R. performed all bioinformatics analysis. K.S. and D.P. provided support with aspects of the network science expertise. F.R, B.A. and V.P. wrote the manuscript. V.P. supervised the project.

Competing interests

Authors declare no competing interests.

References

Acemel, R.D., Lupiáñez, D.G., 2023. Evolution of 3D chromatin organization at different scales. Curr. Opin. Genet. Dev. 78, 102019. https://doi.org/10.1016/j.gde.2022.102019

Achinger-Kawecka, J., Clark, S.J., 2017. Disruption of the 3D Cancer Genome Blueprint. Epigenomics 9, 47–55. https://doi.org/10.2217/epi-2016-0111

Adelman, K., Lis, J.T., 2012. Promoter-proximal pausing of RNA polymerase II: emerging

roles in metazoans. Nat. Rev. Genet. 13, 720–731. https://doi.org/10.1038/nrg3293

Alemu, E.Y., Carl, J.W., Corrada Bravo, H., Hannenhalli, S., 2014. Determinants of expression variability. Nucleic Acids Res. 42, 3503–3514. https://doi.org/10.1093/nar/gkt1364

Athena Aktipis, C., Boddy, A.M., Jansen, G., Hibner, U., Hochberg, M.E., Maley, C.C., Wilkinson, G.S., 2015. Cancer across the tree of life: Cooperation and cheating in multicellularity. Philos. Trans. R. Soc. B Biol. Sci. 370. https://doi.org/10.1098/rstb.2014.0219

Barkai, N., Shilo, B.-Z., 2007. Variability and Robustness in Biomolecular Systems. Mol. Cell 28, 755–760. https://doi.org/10.1016/j.molcel.2007.11.013

Beagan, J.A., Phillips-Cremins, J.E., 2020. On the existence and functionality of topologically associating domains. Nat. Genet. 52, 8–16. https://doi.org/10.1038/s41588-019-0561-1

Benton, M.L., Abraham, A., LaBella, A.L., Abbot, P., Rokas, A., Capra, J.A., 2021. The influence of evolutionary history on human health and disease. Nat. Rev. Genet. 22, 269–283. https://doi.org/10.1038/s41576-020-00305-9

Bird, A., 2002. DNA methylation patterns and epigenetic memory. Genes Dev 16. https://doi.org/10.1101/gad.947102

Bouwman, B.A.M., Crosetto, N., Bienko, M., 2022. RNA gradients: Shapers of 3D genome architecture. Curr. Opin. Cell Biol. 74, 7–12. https://doi.org/10.1016/j.ceb.2021.12.001

Boveri, T., 2008. Concerning the Origin of Malignant Tumours by Theodor Boveri. Translated and annotated by Henry Harris. J. Cell Sci. 121, 1–84. https://doi.org/10.1242/jcs.025742

Brotto, D.B., Siena, Á.D.D., De Barros, I.I., Carvalho, S.D.C.E.S., Muys, B.R., Goedert, L., Cardoso, C., Plaça, J.R., Ramão, A., Squire, J.A., Araujo, L.F., Silva, W.A.D., 2020. Contributions of HOX genes to cancer hallmarks: Enrichment pathway analysis and review. Tumor Biol. 42, 101042832091805. https://doi.org/10.1177/1010428320918050

Burdziak, C., Alonso-Curbelo, D., Walle, T., Reyes, J., Barriga, F.M., Haviv, D., Xie, Y., Zhao, Z., Zhao, C.J., Chen, H.-A., Chaudhary, O., Masilionis, I., Choo, Z.-N., Gao, V., Luan, W., Wuest, A., Ho, Y.-J., Wei, Y., Quail, D.F., Koche, R., Mazutis, L., Chaligné, R., Nawy, T., Lowe, S.W., Pe’er, D., 2023. Epigenetic plasticity cooperates with cell-cell interactions to direct pancreatic tumorigenesis. Science 380, eadd5327. https://doi.org/10.1126/science.add5327

Busser, B.W., Lin, Y., Yang, Y., Zhu, J., Chen, G., Michelson, A.M., 2015. An Orthologous Epigenetic Gene Expression Signature Derived from Differentiating Embryonic Stem Cells Identifies Regulators of Cardiogenesis. PLOS ONE 10, e0141066.

https://doi.org/10.1371/journal.pone.0141066

Bussey, K.J., Cisneros, L.H., Lineweaver, C.H., Davies, P.C.W., 2017. Ancestral gene regulatory networks drive cancer. Proc. Natl. Acad. Sci. U. S. A. 114, 6160–6162. https://doi.org/10.1073/pnas.1706990114

Che, Y., Yang, X., Jia, P., Wang, T., Xu, D., Guo, T., Ye, K., 2022. D^2 Plot, a Matrix of DNA Density and Distance to Periphery, Reveals Functional Genome Regions. Adv. Sci. 9, 2202149. https://doi.org/10.1002/advs.202202149

Chen, L., Ge, B., Casale, F.P., Vasquez, L., Kwan, T., Garrido-Martín, D., Watt, S., Yan, Y., Kundu, K., Ecker, S., Datta, A., Richardson, D., Burden, F., Mead, D., Mann, A.L., Fernandez, J.M., Rowlston, S., Wilder, S.P., Farrow, S., Shao, X., Lambourne, J.J., Redensek, A., Albers, C.A., Amstislavskiy, V., Ashford, S., Berentsen, K., Bomba, L., Bourque, G., Bujold, D., Busche, S., Caron, M., Chen, S.-H., Cheung, W., Delaneau, O., Dermitzakis, E.T., Elding, H., Colgiu, I., Bagger, F.O., Flicek, P., Habibi, E., Iotchkova, V., Janssen-Megens, E., Kim, B., Lehrach, H., Lowy, E., Mandoli, A., Matarese, F., Maurano, M.T., Morris, J.A., Pancaldi, V., Pourfarzad, F., Rehnstrom, K., Rendon, A., Risch, T., Sharifi, N., Simon, M.-M., Sultan, M., Valencia, A., Walter, K., Wang, S.-Y., Frontini, M., Antonarakis, S.E., Clarke, L., Yaspo, M.-L., Beck, S., Guigo, R., Rico, D., Martens, J.H.A., Ouwehand, W.H., Kuijpers, T.W., Paul, D.S., Stunnenberg, H.G., Stegle, O., Downes, K., Pastinen, T., Soranzo, N., 2016. Genetic Drivers of Epigenetic and Transcriptional Variation in Human Immune Cells. Cell 167, 1398-1414.e24. https://doi.org/10.1016/j.cell.2016.10.026

Choy, M.-K., Javierre, B.M., Williams, S.G., Baross, S.L., Liu, Y., Wingett, S.W., Akbarov, A., Wallace, C., Freire-Pritchett, P., Rugg-Gunn, P.J., Spivakov, M., Fraser, P., Keavney, B.D., 2018. Promoter interactome of human embryonic stem cell-derived cardiomyocytes connects GWAS regions to cardiac gene networks. Nat. Commun. 9, 2526. https://doi.org/10.1038/s41467-018-04931-0

Cremer, T., Cremer, C., 2001. Chromosome territories, nuclear architecture and gene regulation in mammalian cells. Nat. Rev. Genet. 2, 292–301. https://doi.org/10.1038/35066075

Csárdi, G., Nepusz, T., Müller, K., Horvát, S., Traag, V., Zanini, F., Noom, D., 2023. igraph for R: R interface of the igraph library for graph theory and network analysis. https://doi.org/10.5281/ZENODO.7682609

De Langen, P., Hammal, F., Guéret, E., Mouren, J.-C., Spinelli, L., Ballester, B., 2023. Characterizing intergenic transcription at RNA polymerase II binding sites in normal and cancer tissues. Cell Genomics 3, 100411. https://doi.org/10.1016/j.xgen.2023.100411

Deng, S., Feng, Y., Pauklin, S., 2022. 3D chromatin architecture and transcription regulation

in cancer. J. Hematol. Oncol.J Hematol Oncol 15, 49. https://doi.org/10.1186/s13045-022-01271-x

Domazet-Lošo, T., Brajković, J., Tautz, D., 2007. A phylostratigraphy approach to uncover the genomic history of major adaptations in metazoan lineages. Trends Genet. 23, 533–539. https://doi.org/10.1016/j.tig.2007.08.014

Domazet-Lošo, T., Tautz, D., 2010. Phylostratigraphic tracking of cancer genes suggests a link to the emergence of multicellularity in metazoa. BMC Biol. 8, 66. https://doi.org/10.1186/1741-7007-8-66

Ecker, S., Chen, L., Pancaldi, V., Bagger, F.O., Fernández, J.M., Carrillo De Santa Pau, E., Juan, D., Mann, A.L., Watt, S., Casale, F.P., Sidiropoulos, N., Rapin, N., Merkel, A., BLUEPRINT Consortium, Stunnenberg, H.G., Stegle, O., Frontini, M., Downes, K., Pastinen, T., Kuijpers, T.W., Rico, D., Valencia, A., Beck, S., Soranzo, N., Paul, D.S., 2017. Genome-wide analysis of differential transcriptional and epigenetic variability across human immune cell types. Genome Biol. 18, 18. https://doi.org/10.1186/s13059-017-1156-8

Ecker, S., Pancaldi, V., Rico, D., Valencia, A., 2015. Higher gene expression variability in the more aggressive subtype of chronic lymphocytic leukemia. Genome Med. 7, 8. https://doi.org/10.1186/s13073-014-0125-z

Ecker, S., Pancaldi, V., Valencia, A., Beck, S., Paul, D.S., 2018a. Epigenetic and Transcriptional Variability Shape Phenotypic Plasticity. BioEssays 40, 1700148. https://doi.org/10.1002/bies.201700148

Ecker, S., Pancaldi, V., Valencia, A., Beck, S., Paul, D.S., 2018b. Epigenetic and Transcriptional Variability Shape Phenotypic Plasticity. BioEssays 40, 1700148. https://doi.org/10.1002/bies.201700148

Feng, Y., Zhang, T., Wang, Y., Xie, M., Ji, X., Luo, X., Huang, W., Xia, L., 2021. Homeobox Genes in Cancers: From Carcinogenesis to Recent Therapeutic Intervention. Front. Oncol. 11, 770428. https://doi.org/10.3389/fonc.2021.770428

Frank, S.A., Yanai, I., 2024. The origin of novel traits in cancer. Trends Cancer S2405803324001456. https://doi.org/10.1016/j.trecan.2024.07.005

Freire-Pritchett, P., Schoenfelder, S., Várnai, C., Wingett, S.W., Cairns, J., Collier, A.J., García-Vílchez, R., Furlan-Magaril, M., Osborne, C.S., Fraser, P., Rugg-Gunn, P.J., Spivakov, M., 2017. Global reorganisation of cis-regulatory units upon lineage commitment of human embryonic stem cells. eLife 6, e21926. https://doi.org/10.7554/eLife.21926

Gentile, C., Kmita, M., 2020. Polycomb Repressive Complexes in *Hox* Gene Regulation: Silencing and Beyond: The Functional Dynamics of Polycomb Repressive Complexes in *Hox* Gene Regulation. BioEssays 42, 1900249.

https://doi.org/10.1002/bies.201900249

Hagai, T., Chen, X., Miragaia, R.J., Rostom, R., Gomes, T., Kunowska, N., Henriksson, J., Park, J.-E., Proserpio, V., Donati, G., Bossini-Castillo, L., Vieira Braga, F.A., Naamati, G., Fletcher, J., Stephenson, E., Vegh, P., Trynka, G., Kondova, I., Dennis, M., Haniffa, M., Nourmohammad, A., Lässig, M., Teichmann, S.A., 2018. Gene expression variability across cells and species shapes innate immunity. Nature 563, 197–202. https://doi.org/10.1038/s41586-018-0657-2

Hanahan, D., 2022. Hallmarks of Cancer: New Dimensions. Cancer Discov. 12, 31–46. https://doi.org/10.1158/2159-8290.CD-21-1059

Hehmeyer, J., Spitz, F., Marlow, H., 2023. Shifting landscapes: the role of 3D genomic organizations in gene regulatory strategies. Curr. Opin. Genet. Dev. 81, 102064. https://doi.org/10.1016/j.gde.2023.102064

Henikoff, S., 2023. The epigenetic landscape: An evolving concept. Front. Epigenetics Epigenomics 1, 1176449. https://doi.org/10.3389/freae.2023.1176449

Hoencamp, C., Dudchenko, O., Elbatsh, A.M.O., Brahmachari, S., Raaijmakers, J.A., Van Schaik, T., Sedeño Cacciatore, Á., Contessoto, V.G., Van Heesbeen, R.G.H.P., Van Den Broek, B., Mhaskar, A.N., Teunissen, H., St Hilaire, B.G., Weisz, D., Omer, A.D., Pham, M., Colaric, Z., Yang, Z., Rao, S.S.P., Mitra, N., Lui, C., Yao, W., Khan, R., Moroz, L.L., Kohn, A., St. Leger, J., Mena, A., Holcroft, K., Gambetta, M.C., Lim, F., Farley, E., Stein, N., Haddad, A., Chauss, D., Mutlu, A.S., Wang, M.C., Young, N.D., Hildebrandt, E., Cheng, H.H., Knight, C.J., Burnham, T.L.U., Hovel, K.A., Beel, A.J., Mattei, P.-J., Kornberg, R.D., Warren, W.C., Cary, G., Gómez-Skarmeta, J.L., Hinman, V., Lindblad-Toh, K., Di Palma, F., Maeshima, K., Multani, A.S., Pathak, S., Nel-Themaat, L., Behringer, R.R., Kaur, P., Medema, R.H., Van Steensel, B., De Wit, E., Onuchic, J.N., Di Pierro, M., Lieberman Aiden, E., Rowland, B.D., 2021. 3D genomics across the tree of life reveals condensin II as a determinant of architecture type. Science 372, 984–989. https://doi.org/10.1126/science.abe2218

Hunter, M.V., Montal, E., Ma, Y., Moncada, R., Yanai, I., Koche, R.P., White, R.M., 2024. Mechanical confinement governs phenotypic plasticity in melanoma. https://doi.org/10.1101/2024.01.30.577120

James, C., Trevisan-Herraz, M., Juan, D., Rico, D., 2021. Vertebrate whole genome duplications shaped the current 3D genome architecture (preprint). Genomics. https://doi.org/10.1101/2021.06.11.448047

Jang, S.H., Lee, S., Chung, H.Y., 2015. Characterization of Leukemia-Inducing Genes Using a Proto-Oncogene/Homeobox Gene Retroviral Human cDNA Library in a Mouse In Vivo Model. PLOS ONE 10, e0143240. https://doi.org/10.1371/journal.pone.0143240

Javierre, B.M., Burren, O.S., Wilder, S.P., Kreuzhuber, R., Hill, S.M., Sewitz, S., Cairns, J.,

Wingett, S.W., Várnai, C., Thiecke, M.J., Burden, F., Farrow, S., Cutler, A.J., Rehnström, K., Downes, K., Grassi, L., Kostadima, M., Freire-Pritchett, P., Wang, F., Martens, J.H., Kim, B., Sharifi, N., Janssen-Megens, E.M., Yaspo, M.-L., Linser, M., Kovacsovics, A., Clarke, L., Richardson, D., Datta, A., Flicek, P., Stunnenberg, H.G., Todd, J.A., Zerbino, D.R., Stegle, O., Ouwehand, W.H., Frontini, M., Wallace, C., Spivakov, M., Fraser, P., 2016. Lineage-Specific Genome Architecture Links Enhancers and Non-coding Disease Variants to Target Gene Promoters. Cell 167, 1369-1384.e19. https://doi.org/10.1016/j.cell.2016.09.037

Jodkowska, K., Pancaldi, V., Rigau, M., Almeida, R., Fernández-Justel, J.M., Graña-Castro, O., Rodríguez-Acebes, S., Rubio-Camarillo, M., Carrillo-de Santa Pau, E., Pisano, D., Al-Shahrour, F., Valencia, A., Gómez, M., Méndez, J., 2022. 3D chromatin connectivity underlies replication origin efficiency in mouse embryonic stem cells. Nucleic Acids Res. 50, 12149–12165. https://doi.org/10.1093/nar/gkac1111

Juan, D., Rico, D., Marques-Bonet, T., Fernández-Capetillo, Ó., Valencia, A., 2013. Late-replicating CNVs as a source of new genes. Biol. Open 2, 1402–1411. https://doi.org/10.1242/bio.20136924

Kar, G., Kim, J.K., Kolodziejczyk, A.A., Natarajan, K.N., Torlai Triglia, E., Mifsud, B., Elderkin, S., Marioni, J.C., Pombo, A., Teichmann, S.A., 2017. Flipping between Polycomb repressed and active transcriptional states introduces noise in gene expression. Nat. Commun. 8, 36. https://doi.org/10.1038/s41467-017-00052-2

Kim, J.J., Kingston, R.E., 2022. Context-specific Polycomb mechanisms in development. Nat. Rev. Genet. 23, 680–695. https://doi.org/10.1038/s41576-022-00499-0

Kind, J., Pagie, L., de Vries, S.S., Nahidiazar, L., Dey, S.S., Bienko, M., Zhan, Y., Lajoie, B., de Graaf, C.A., Amendola, M., Fudenberg, G., Imakaev, M., Mirny, L.A., Jalink, K., Dekker, J., van Oudenaarden, A., van Steensel, B., 2015. Genome-wide Maps of Nuclear Lamina Interactions in Single Human Cells. Cell 163, 134–147. https://doi.org/10.1016/j.cell.2015.08.040

Li, H., Durbin, R., 2010. Fast and accurate long-read alignment with Burrows-Wheeler transform. Bioinformatics 26, 589–595. https://doi.org/10.1093/bioinformatics/btp698

Li, H., Handsaker, B., Wysoker, A., Fennell, T., Ruan, J., Homer, N., Marth, G., Abecasis, G., Durbin, R., 2009. The Sequence Alignment/Map format and SAMtools. Bioinformatics 25, 2078–2079. https://doi.org/10.1093/bioinformatics/btp352

Li Shen, M.S. <Shenli S.C., 2017. GeneOverlap. https://doi.org/10.18129/B9.BIOC.GENEOVERLAP

Lineweaver, C.H., Bussey, K.J., Blackburn, A.C., Davies, P.C.W., 2021. Cancer progression as a sequence of atavistic reversions. BioEssays 43, 2000305. https://doi.org/10.1002/bies.202000305

Madrid-Mencía, M., Raineri, E., Cao, T.B.N., Pancaldi, V., 2020. Using GARDEN-NET and ChAseR to explore human haematopoietic 3D chromatin interaction networks. Nucleic Acids Res. 48, 4066–4080. https://doi.org/10.1093/nar/gkaa159

Mann, R.S., Glassford, W.J., 2024. Hox genes: The original body builders. Semin. Cell Dev. Biol. 152–153, 1–3. https://doi.org/10.1016/j.semcdb.2023.05.005

Meaburn, K.J., Gudla, P.R., Khan, S., Lockett, S.J., Misteli, T., 2009. Disease-specific gene repositioning in breast cancer. J. Cell Biol. 187, 801–812. https://doi.org/10.1083/jcb.200909127

Messina, O., Raynal, F., Gurgo, J., Fiche, J.-B., Pancaldi, V., Nollmann, M., 2023. 3D chromatin interactions involving Drosophila insulators are infrequent but preferential and arise before TADs and transcription. Nat. Commun. 14, 6678. https://doi.org/10.1038/s41467-023-42485-y

Misteli, T., 2020. The Self-Organizing Genome: Principles of Genome Architecture and Function. Cell 183, 28–45. https://doi.org/10.1016/j.cell.2020.09.014

Misteli, T., 2007. Beyond the Sequence: Cellular Organization of Genome Function. Cell 128, 787–800. https://doi.org/10.1016/j.cell.2007.01.028

Murphy, S.E., Boettiger, A.N., 2024. Polycomb repression of Hox genes involves spatial feedback but not domain compaction or phase transition. Nat. Genet. 56, 493–504. https://doi.org/10.1038/s41588-024-01661-6

Nakatani, T., Schauer, T., Altamirano-Pacheco, L., Klein, K.N., Ettinger, A., Pal, M., Gilbert, D.M., Torres-Padilla, M.-E., 2024. Emergence of replication timing during early mammalian development. Nature 625, 401–409. https://doi.org/10.1038/s41586-023-06872-1

Pancaldi, V., 2023. Network models of chromatin structure. Curr. Opin. Genet. Dev. 80, 102051. https://doi.org/10.1016/j.gde.2023.102051

Pancaldi, V., 2021. Chromatin Network Analyses: Towards Structure-Function Relationships in Epigenomics. Front. Bioinforma. 1, 742216. https://doi.org/10.3389/fbinf.2021.742216

Pancaldi, V., Carrillo-de-Santa-Pau, E., Javierre, B.M., Juan, D., Fraser, P., Spivakov, M., Valencia, A., Rico, D., 2016. Integrating epigenomic data and 3D genomic structure with a new measure of chromatin assortativity. Genome Biol. 17, 152. https://doi.org/10.1186/s13059-016-1003-3

Pancaldi, V., Schubert, F., Bähler, J., 2010. Meta-analysis of genome regulation and expression variability across hundreds of environmental and genetic perturbations in fission yeast. Mol BioSyst 6, 543–552. https://doi.org/10.1039/B913876P

Papadogkonas, G., Papamatheakis, D.-A., Spilianakis, C., 2022. 3D Genome Organization as an Epigenetic Determinant of Transcription Regulation in T Cells. Front. Immunol.

13, 921375. https://doi.org/10.3389/fimmu.2022.921375

Parreno, V., Loubiere, V., Schuettengruber, B., Fritsch, L., Rawal, C.C., Erokhin, M., Győrffy, B., Normanno, D., Di Stefano, M., Moreaux, J., Butova, N.L., Chiolo, I., Chetverina, D., Martinez, A.-M., Cavalli, G., 2024. Transient loss of Polycomb components induces an epigenetic cancer fate. Nature 629, 688–696. https://doi.org/10.1038/s41586-024-07328-w

Patani, H., Rushton, M.D., Higham, J., Teijeiro, S.A., Oxley, D., Cutillas, P., Sproul, D., Ficz, G., 2020. Transition to naïve human pluripotency mirrors pan-cancer DNA hypermethylation. Nat. Commun. 11, 3671. https://doi.org/10.1038/s41467-020-17269-3

Pope, B.D., Ryba, T., Dileep, V., Yue, F., Wu, W., Denas, O., Vera, D.L., Wang, Y., Hansen, R.S., Canfield, T.K., Thurman, R.E., Cheng, Y., Gülsoy, G., Dennis, J.H., Snyder, M.P., Stamatoyannopoulos, J.A., Taylor, J., Hardison, R.C., Kahveci, T., Ren, B., Gilbert, D.M., 2014. Topologically associating domains are stable units of replication-timing regulation. Nature 515, 402–405. https://doi.org/10.1038/nature13986

Prorok, P., Forouzanfar, F., Murugarren, N., Peiffer, I., Charton, R., Akerman, I., Méchali, M., 2023. Loss of Ezh2 function remodels the DNA replication initiation landscape. Cell Rep. 42, 112280. https://doi.org/10.1016/j.celrep.2023.112280

Reddy, K.L., Zullo, J.M., Bertolino, E., Singh, H., 2008. Transcriptional repression mediated by repositioning of genes to the nuclear lamina. Nature 452, 243–247. https://doi.org/10.1038/nature06727

Ritchie, M.E., Phipson, B., Wu, D., Hu, Y., Law, C.W., Shi, W., Smyth, G.K., 2015. limma powers differential expression analyses for RNA-sequencing and microarray studies. Nucleic Acids Res. 43, e47–e47. https://doi.org/10.1093/nar/gkv007

Sandhu, K.S., Li, G., Poh, H.M., Quek, Y.L.K., Sia, Y.Y., Peh, S.Q., Mulawadi, F.H., Lim, J., Sikic, M., Menghi, F., Thalamuthu, A., Sung, W.K., Ruan, X., Fullwood, M.J., Liu, E., Csermely, P., Ruan, Y., 2012. Large-Scale Functional Organization of Long-Range Chromatin Interaction Networks. Cell Rep. 2, 1207–1219. https://doi.org/10.1016/j.celrep.2012.09.022

Schoenfelder, S., Sugar, R., Dimond, A., Javierre, B.-M., Armstrong, H., Mifsud, B., Dimitrova, E., Matheson, L., Tavares-Cadete, F., Furlan-Magaril, M., Segonds-Pichon, A., Jurkowski, W., Wingett, S.W., Tabbada, K., Andrews, S., Herman, B., LeProust, E., Osborne, C.S., Koseki, H., Fraser, P., Luscombe, N.M., Elderkin, S., 2015. Polycomb repressive complex PRC1 spatially constrains the mouse embryonic stem cell genome. Nat. Genet. 47, 1179–1186. https://doi.org/10.1038/ng.3393

Schoenhals, M., Kassambara, A., Vos, J.D., Hose, D., Moreaux, J., Klein, B., 2009. Embryonic stem cell markers expression in cancers. Biochem. Biophys. Res. Commun. 383, 157–162. https://doi.org/10.1016/j.bbrc.2009.02.156

Seufert, I., Gerosa, I., Varamogianni-Mamatsi, V., Vladimirova, A., Sen, E., Mantz, S., Rademacher, A., Schumacher, S., Liakopoulos, P., Kolovos, P., Anders, S., Mallm, J.-P., Papantonis, A., Rippe, K., 2024. Two distinct chromatin modules regulate proinflammatory gene expression. https://doi.org/10.1101/2024.08.03.606159

Sigalova, O.M., Shaeiri, A., Forneris, M., Furlong, E.E., Zaugg, J.B., 2020. Predictive features of gene expression variation reveal mechanistic link with differential expression. Mol. Syst. Biol. 16, e9539. https://doi.org/10.15252/msb.20209539

Sima, J., Gilbert, D.M., 2014. Complex correlations: replication timing and mutational landscapes during cancer and genome evolution. Curr. Opin. Genet. Dev. 25, 93–100. https://doi.org/10.1016/j.gde.2013.11.022

Sloan, C.A., Chan, E.T., Davidson, J.M., Malladi, V.S., Strattan, J.S., Hitz, B.C., Gabdank, I., Narayanan, A.K., Ho, M., Lee, B.T., Rowe, L.D., Dreszer, T.R., Roe, G., Podduturi, N.R., Tanaka, F., Hong, E.L., Cherry, J.M., 2016. ENCODE data at the ENCODE portal. Nucleic Acids Res. 44, D726–D732. https://doi.org/10.1093/nar/gkv1160

Smith, C.L., Poleshko, A., Epstein, J.A., 2021. The nuclear periphery is a scaffold for tissue-specific enhancers. Nucleic Acids Res. 49, 6181–6195. https://doi.org/10.1093/nar/gkab392

Stefansson, O.A., Sigurpalsdottir, B.D., Rognvaldsson, S., Halldorsson, G.H., Juliusson, K., Sveinbjornsson, G., Gunnarsson, B., Beyter, D., Jonsson, H., Gudjonsson, S.A., Olafsdottir, T.A., Saevarsdottir, S., Magnusson, M.K., Lund, S.H., Tragante, V., Oddsson, A., Hardarson, M.T., Eggertsson, H.P., Gudmundsson, R.L., Sverrisson, S., Frigge, M.L., Zink, F., Holm, H., Stefansson, H., Rafnar, T., Jonsdottir, I., Sulem, P., Helgason, A., Gudbjartsson, D.F., Halldorsson, B.V., Thorsteinsdottir, U., Stefansson, K., 2024. The correlation between CpG methylation and gene expression is driven by sequence variants. Nat. Genet. https://doi.org/10.1038/s41588-024-01851-2

Stempor, P., Ahringer, J., 2016. SeqPlots - Interactive software for exploratory data analyses, pattern discovery and visualization in genomics. Wellcome Open Res. 1, 14. https://doi.org/10.12688/wellcomeopenres.10004.1

Takizawa, T., Meaburn, K.J., Misteli, T., 2008. The Meaning of Gene Positioning. Cell 135, 9–13. https://doi.org/10.1016/j.cell.2008.09.026

Trigos, A.S., Pearson, R.B., Papenfuss, A.T., Goode, D.L., 2019. Somatic mutations in early metazoan genes disrupt regulatory links between unicellular and multicellular genes in cancer. eLife 8, 1–28. https://doi.org/10.7554/eLife.40947

Trigos, A.S., Pearson, R.B., Papenfuss, A.T., Goode, D.L., 2017. Altered interactions

between unicellular and multicellular genes drive hallmarks of transformation in a diverse range of solid tumors. Proc. Natl. Acad. Sci. U. S. A. 114, 6406–6411. https://doi.org/10.1073/pnas.1617743114

Van Steensel, B., Belmont, A.S., 2017. Lamina-Associated Domains: Links with Chromosome Architecture, Heterochromatin, and Gene Repression. Cell 169, 780–791. https://doi.org/10.1016/j.cell.2017.04.022

Wang, M., Sunkel, B.D., Ray, W.C., Stanton, B.Z., 2022. Chromatin structure in cancer. BMC Mol. Cell Biol. 23, 35. https://doi.org/10.1186/s12860-022-00433-6

Wu, T., Hu, E., Xu, S., Chen, M., Guo, P., Dai, Z., Feng, T., Zhou, L., Tang, W., Zhan, L., Fu, X., Liu, S., Bo, X., Yu, G., 2021. clusterProfiler 4.0: A universal enrichment tool for interpreting omics data. The Innovation 2, 100141. https://doi.org/10.1016/j.xinn.2021.100141

Yamanaka, Y., Hamidi, S., Yoshioka-Kobayashi, K., Munira, S., Sunadome, K., Zhang, Y., Kurokawa, Y., Ericsson, R., Mieda, A., Thompson, J.L., Kerwin, J., Lisgo, S., Yamamoto, T., Moris, N., Martinez-Arias, A., Tsujimura, T., Alev, C., 2023. Reconstituting human somitogenesis in vitro. Nature 614, 509–520. https://doi.org/10.1038/s41586-022-05649-2

Yin, H., Li, M., Xia, L., He, C., Zhang, Z., 2019. Computational determination of gene age and characterization of evolutionary dynamics in human. Brief. Bioinform. 20, 2141–2149. https://doi.org/10.1093/bib/bby074

Yin, H., Ma, L., Wang, G., Li, M., Zhang, Z., 2016. Old genes experience stronger translational selection than young genes. Gene 590, 29–34. https://doi.org/10.1016/j.gene.2016.05.041

Yu, G., Wang, L.-G., He, Q.-Y., 2015. ChIPseeker: an R/Bioconductor package for ChIP peak annotation, comparison and visualization. Bioinformatics 31, 2382–2383. https://doi.org/10.1093/bioinformatics/btv145

Zhang, S., Übelmesser, N., Barbieri, M., Papantonis, A., 2023. Enhancer–promoter contact formation requires RNAPII and antagonizes loop extrusion. Nat. Genet. 55, 832–840. https://doi.org/10.1038/s41588-023-01364-4

Zhang, S., Übelmesser, N., Josipovic, N., Forte, G., Slotman, J.A., Chiang, M., Gothe, H.J., Gusmao, E.G., Becker, C., Altmüller, J., Houtsmuller, A.B., Roukos, V., Wendt, K.S., Marenduzzo, D., Papantonis, A., 2021. RNA polymerase II is required for spatial chromatin reorganization following exit from mitosis. Sci. Adv. 7, eabg8205. https://doi.org/10.1126/sciadv.abg8205

Zhang, Y., Liu, T., Meyer, C.A., Eeckhoute, J., Johnson, D.S., Bernstein, B.E., Nusbaum, C., Myers, R.M., Brown, M., Li, W., Liu, X.S., 2008. Model-based Analysis of ChIP-Seq (MACS). Genome Biol. 9, R137. https://doi.org/10.1186/gb-2008-9-9-r137

Zheng, H., Xie, W., 2019. The role of 3D genome organization in development and cell differentiation. Nat. Rev. Mol. Cell Biol. 20, 535–550. https://doi.org/10.1038/s41580-019-0132-4

Supplementary Figures

Supplementary Figure 1

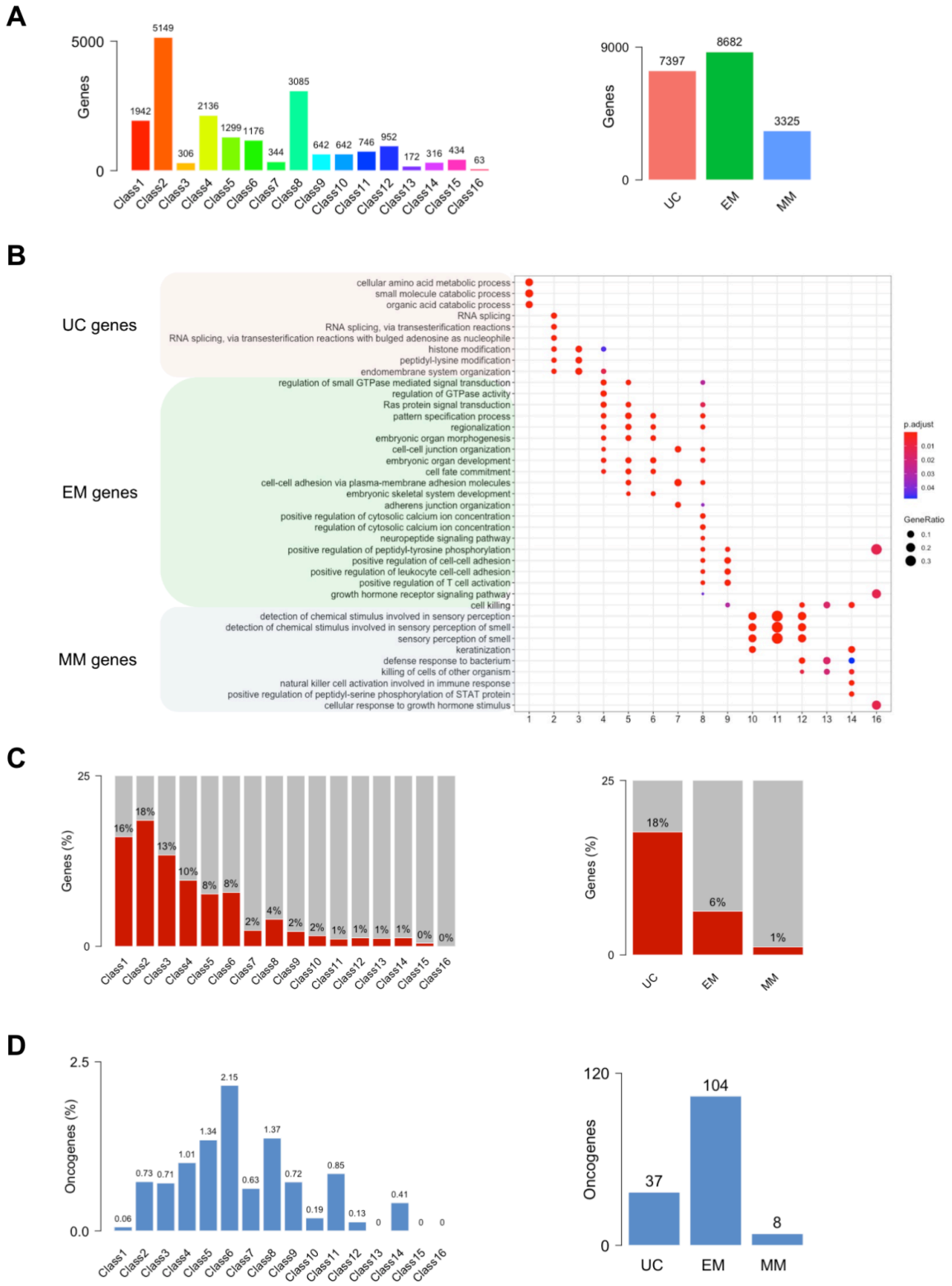

E

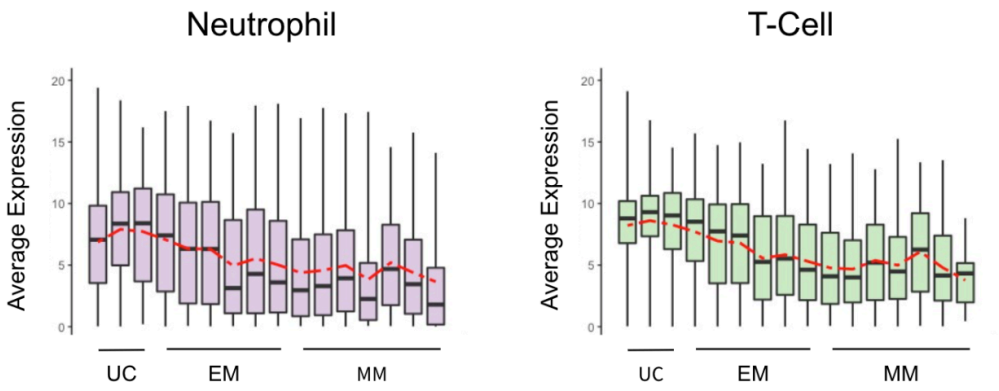
Neutrophil
T-Cell
Average Expression
20
15
10
5
0
UC
EM
MM

F

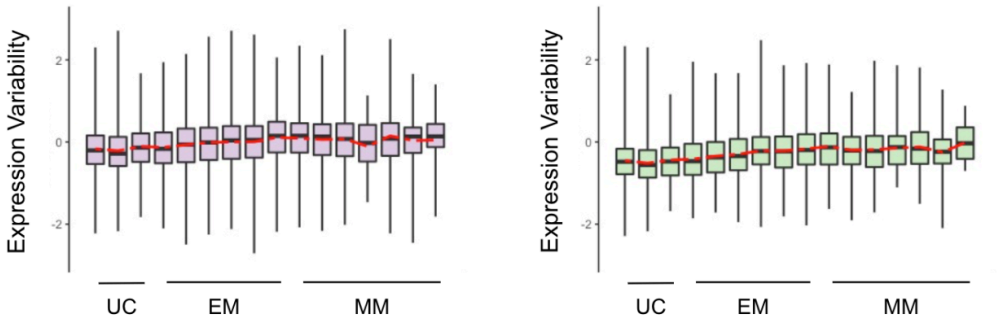
Expression Variability
2
0
-2
UC
EM
MM

G

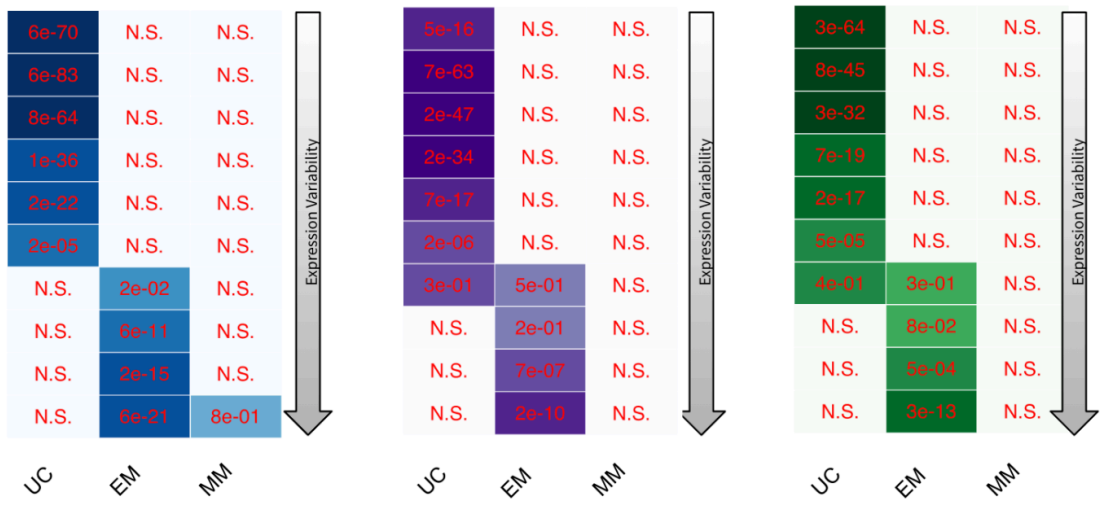
6e-70 N.S. N.S.
6e-83 N.S. N.S.
8e-64 N.S. N.S.
1e-36 N.S. N.S.
2e-22 N.S. N.S.
2e-05 N.S. N.S.
N.S. 2e-02 N.S.
N.S. 6e-11 N.S.
N.S. 2e-15 N.S.
N.S. 6e-21 8e-01
5e-16 N.S. N.S.
7e-63 N.S. N.S.
2e-47 N.S. N.S.
2e-34 N.S. N.S.
7e-17 N.S. N.S.
2e-06 N.S. N.S.
3e-01 5e-01 N.S.
N.S. 2e-01 N.S.
N.S. 7e-07 N.S.
N.S. 2e-10 N.S.
3e-64 N.S. N.S.
8e-45 N.S. N.S.
3e-32 N.S. N.S.
7e-19 N.S. N.S.
2e-17 N.S. N.S.
5e-05 N.S. N.S.
4e-01 3e-01 N.S.
N.S. 8e-02 N.S.
N.S. 5e-04 N.S.
N.S. 3e-13 N.S.
Expression Variability
UC EM MM

H

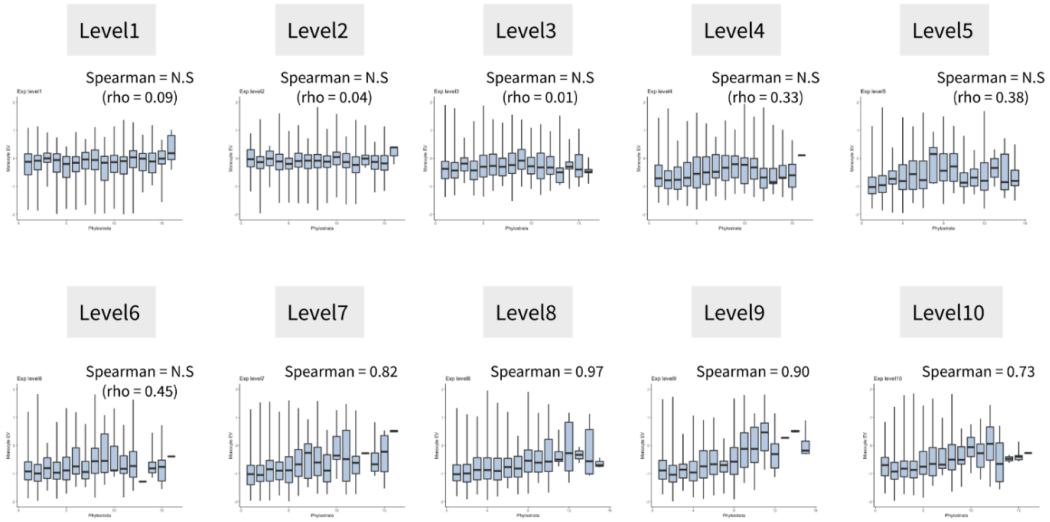
Level1
Spearman = N.S
(rho = 0.09)
Level2
Spearman = N.S
(rho = 0.04)
Level3
Spearman = N.S
(rho = 0.01)
Level4
Spearman = N.S
(rho = 0.33)
Level5
Spearman = N.S
(rho = 0.38)
Level6
Spearman = N.S
(rho = 0.45)
Level7
Spearman = 0.82
Level8
Spearman = 0.97
Level9
Spearman = 0.90
Level10
Spearman = 0.73

I

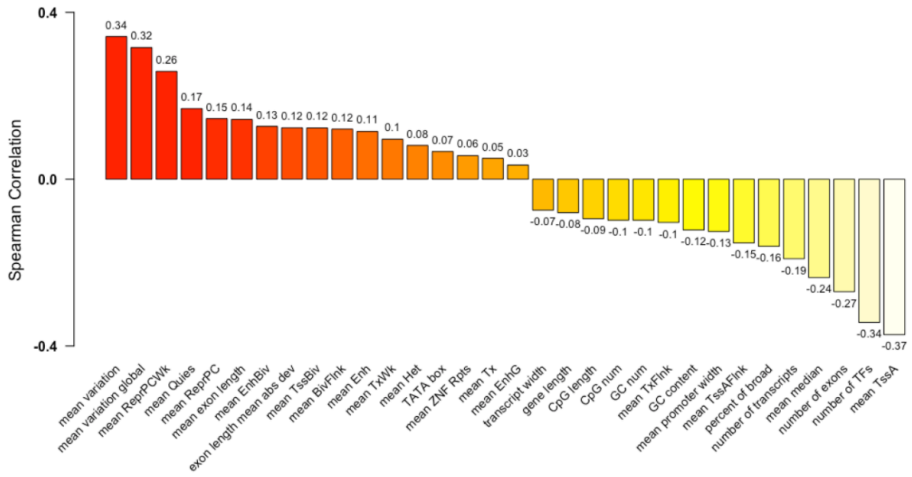
Spearman Correlation
0.4
0.0
-0.4
0.34
0.32
0.26
0.17
0.15
0.14
0.13
0.12
0.12
0.12
0.11
0.1
0.08
0.07
0.06
0.05
0.03
-0.07
-0.08
-0.09
-0.1
-0.1
-0.1
-0.12
-0.13
-0.15
-0.16
-0.19
-0.24
-0.27
-0.34
-0.37
mean variation
mean variation global
mean RepPCWk
mean Ques
mean RepPC
mean exon length
mean EnhBiv
exon length mean abs dev
mean TssBiv
mean BivFlnk
mean Enh
mean TxWk
mean Het
TATA box
mean ZNF Rpts
mean Tx
mean EnhG
transcript width
gene length
CpG length
CpG num
GC num
mean TxFlnk
GC content
mean promoter width
mean TssAFlnk
percent of broad
number of transcripts
mean median
number of exons
number of TFs
mean TssA

J

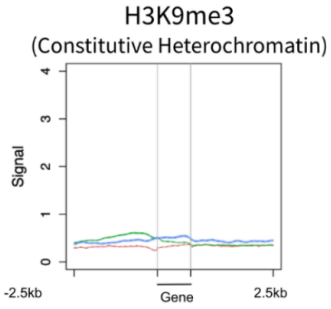
H3K9me3
(Constitutive Heterochromatin)
Signal
0
1
2
3
4
-2.5kb
Gene
2.5kb

K

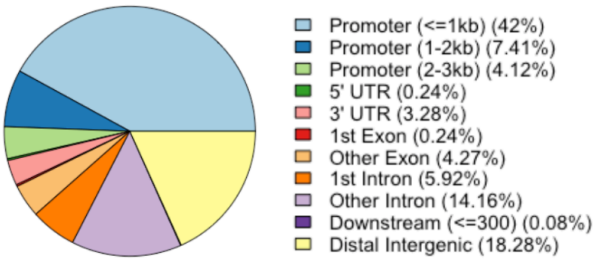
Promoter (<=1kb) (42%)
Promoter (1-2kb) (7.41%)
Promoter (2-3kb) (4.12%)
5' UTR (0.24%)
3' UTR (3.28%)
1st Exon (0.24%)
Other Exon (4.27%)
1st Intron (5.92%)
Other Intron (14.16%)
Downstream (<=300) (0.08%)
Distal Intergenic (18.28%)

Supplementary Fig1. (related to Fig.1)

A) Number of genes in each phylostratum (left) and in each main age class (right). **B**) Gene Ontology enrichment of genes from each phylostratum. **C**) Proportion of housekeeping genes in each phylostratum (left) and in each main age class (right). **D**) Proportion of Leukemia proto-oncogenes in each phylostratum (left) and in each main age class (right). Dataset from Jang *et al*., 2015. **E**) Boxplot of average inter-individual gene expression levels in Neutrophil (left) and T-Cell (right) across 16 gene age classes (Spearman test in neutrophil, Rho = -0.88, *p*-value < 2.2e-16. Spearman test in t-cell, Rho -0.85, *p*-value = 1.023e-05). **F**) Boxplots of inter-individual expression variability in Neutrophil (left) and T-Cell (right) across 16 gene age classes (Spearman test in neutrophil, Rho = 0.74, *p*-value = 0.001703. Spearman test in t-cell, Rho = 0.84, *p*-value = 1.932e-05). **G**) Fisher's Exact Tests of 10 EV decile levels and 3 main gene ages in Monocyte, Neutrophil and T-Cell, from left to right. Color shades show Jaccard index. This confirms the link between EV and gene evolutionary ages. **H**) Boxplots of inter-individual expression variability in Monocyte across the 16 phylostrata for 10 gene expression variability level classes. **I**) Spearman correlations of various DNA variability properties with 16 gene age classes. **J**) Average H3K9me3 profile in Monocyte around the 3 main gene age classes (Red Unicellular genes, Green Early metazoan genes, Blue Mammal Specific genes) (Sigalova et al., 2020). **K**) Genomic localisations of all detected CpG islands in monocytes.

Supplementary Figure 2

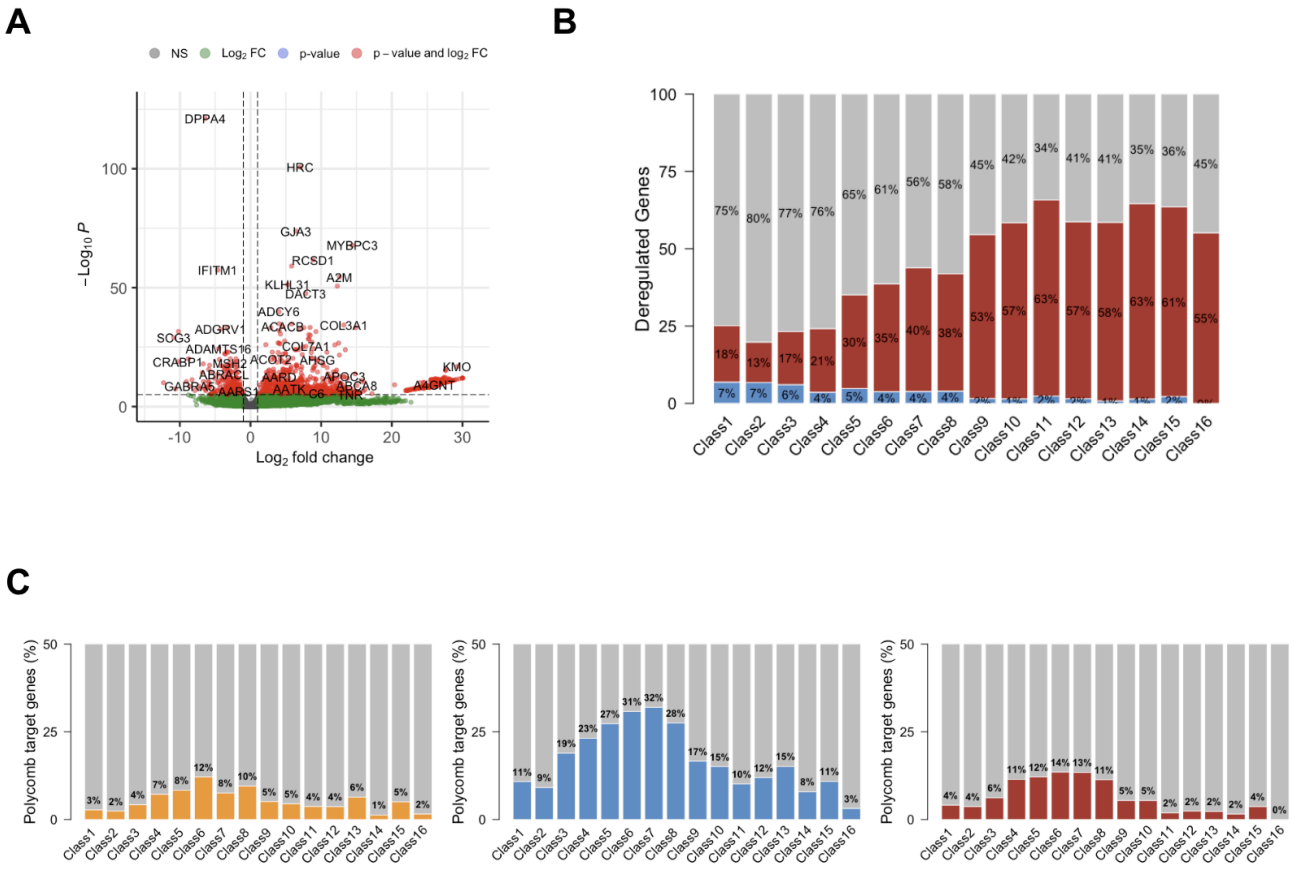

Supplementary Fig2. (related to Fig.2)

A) Volcano plot of differentially expressed genes in Cardiomyocyte compared to hESC. **B**) Proportion of Down (blue), Up (red) and non (grey) deregulated genes in Cardiomyocyte compared to hESC across the 16 gene age categories. **C**) Proportion of Polycomb target genes across the 16 gene age categories in hESC (left), B-cell (middle) and CLL (right).

Supplementary Figure 3

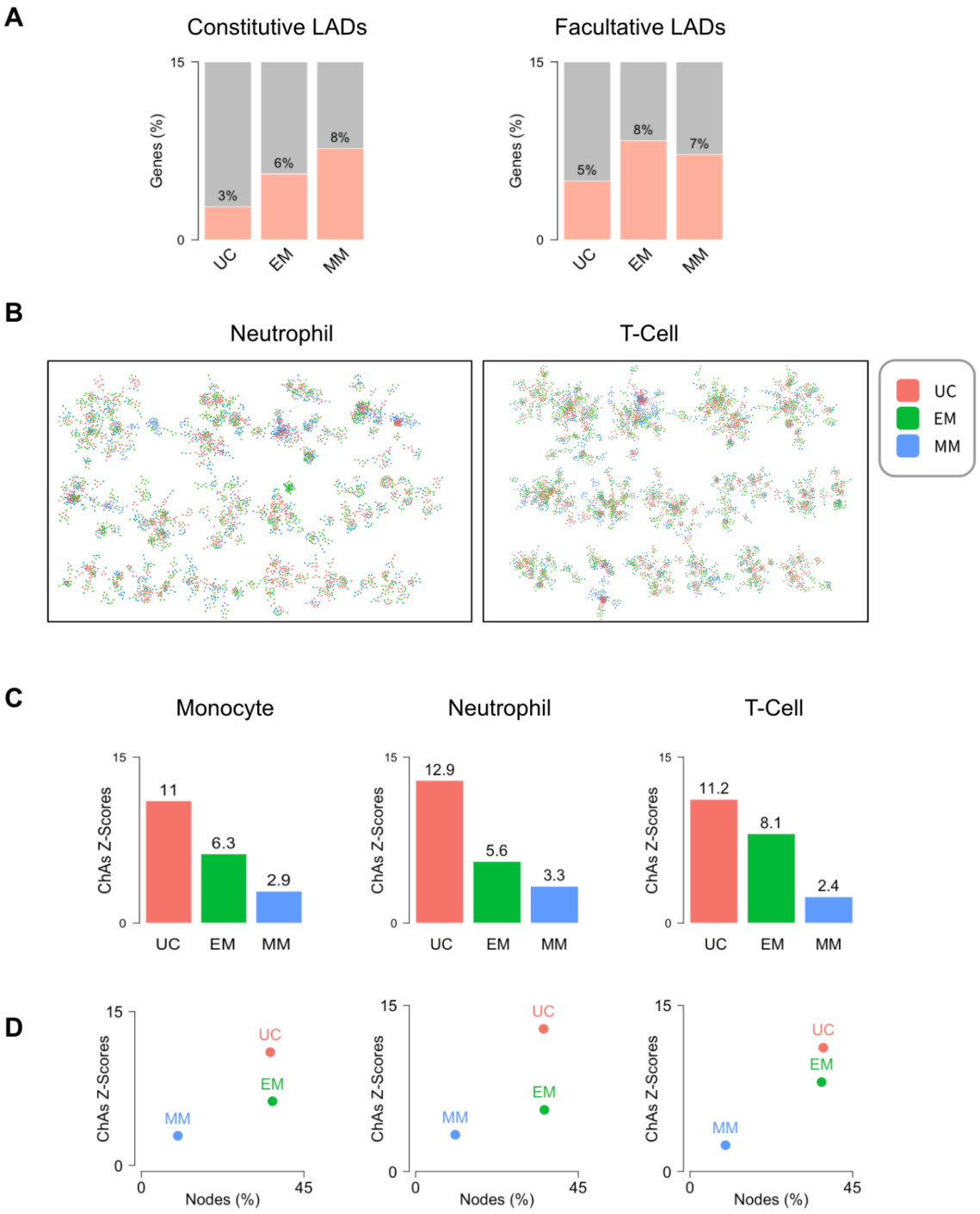

E

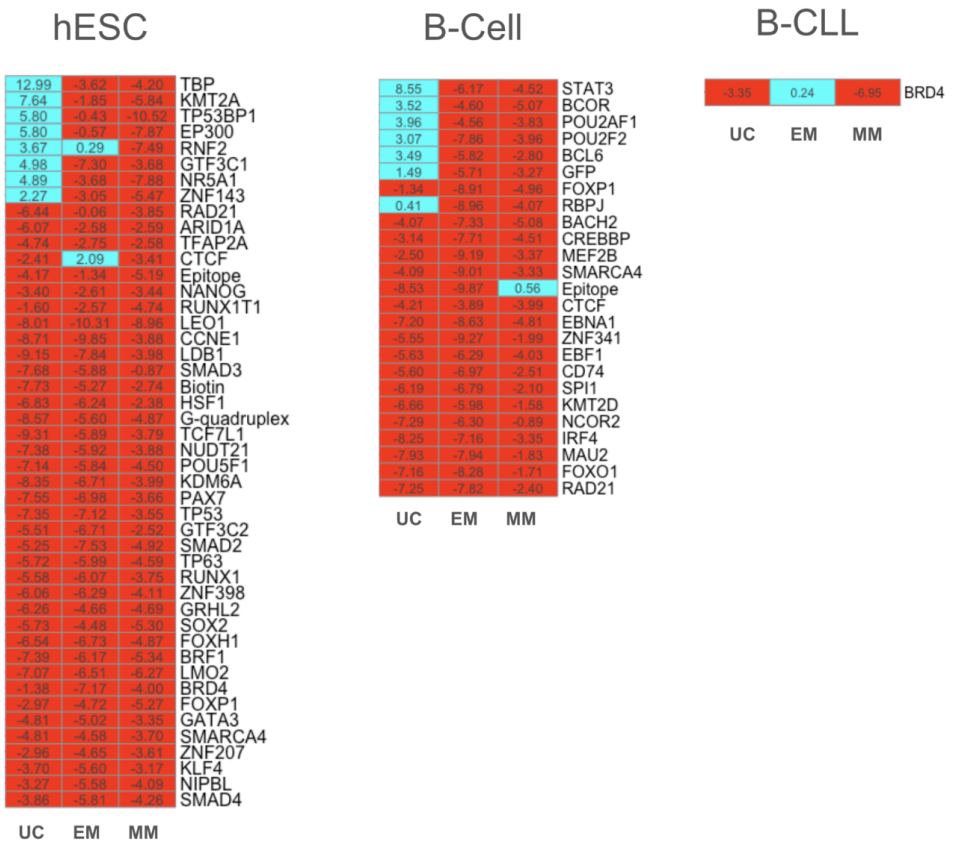

Supplementary Fig3. (related to Fig.3)

A) Overlaps with Lamina Associated Domains (LADs) annotated in multiple cell lines (Kind et al., 2015) for genes belonging to the different age classes. **B**) Visualizations of the 3D promoter-promoter interaction networks in neutrophil (left) and T-cell (right) with node color representing gene age classes (red = UC, green = EM, blue = MM). **C**) ChAs z-scores compared amongst the 3 age classes in monocyte, neutrophil and T-cell promoter-promoter interaction networks. **D**) ChAs z-scores and related feature abundance of the 3 age classes in monocyte, neutrophil and T-cell promoter-promoter interaction networks. **E**) ΔChAs z-scores matrix of several transcription factors and chromatin features in hESC, B-Cell, and B-CLL. Colors represent ΔChAs > 0 in cyan and ΔChAs < 0 in red.